Università degli Studi di Torino
DIPARTIMENTO DI FISICA

# Scalers and solar activity

**Carla Taricco**[1,2]
Cecilia Dionese[1], Salvatore Mancuso[3],
Martin Schimassek[4,5] and Roberto Mussa[2]

*1 Dipartimento di Fisica, Università degli Studi di Torino, Via Pietro Giuria 1, Torino, 10125, Italy*
*2 INFN-Sezione di Torino, Via Pietro Giuria 1, Torino, 10125, Italy*
*3 INAF – Osservatorio Astrofisico di Torino, Via Osservatorio 20, Pino Torinese, 10025, Italy*
*4 IJCLab (Laboratoire de Physique des 2 Infinis Irène Joliot-Curie)*
*5 CNRS/IN2P3, Université Paris-Saclay, Orsay, France*

**Meeting Auger Italia - Torino, 4/2/2025**

# SUMMARY

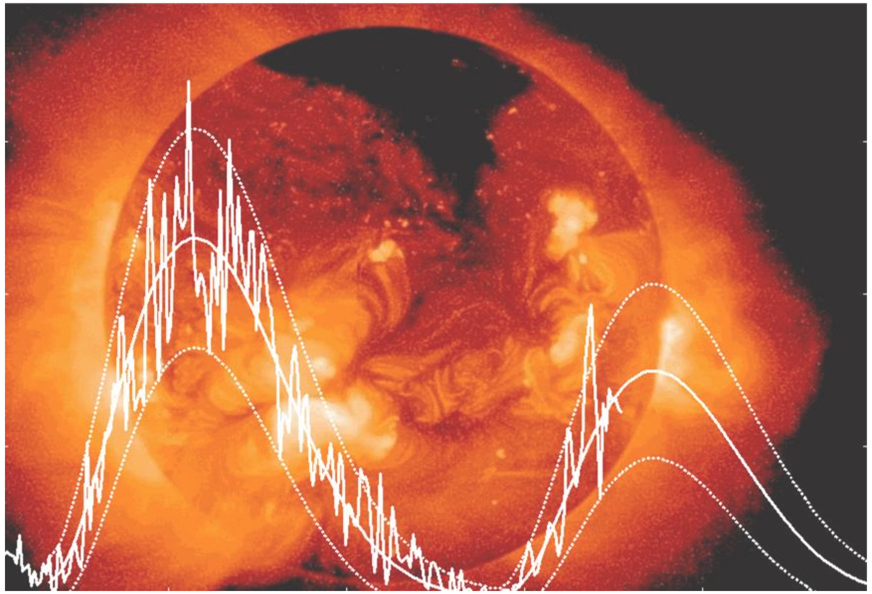

1. Scalers time series, its spectral analysis and comparison with sunspot area and sunspot number series (ApJ sumitted – ICRC2025)
2. Comparison with other proxies of solar activity (in preparation)
3. Future plans and work in progress

# THE SCALER TIME SERIES

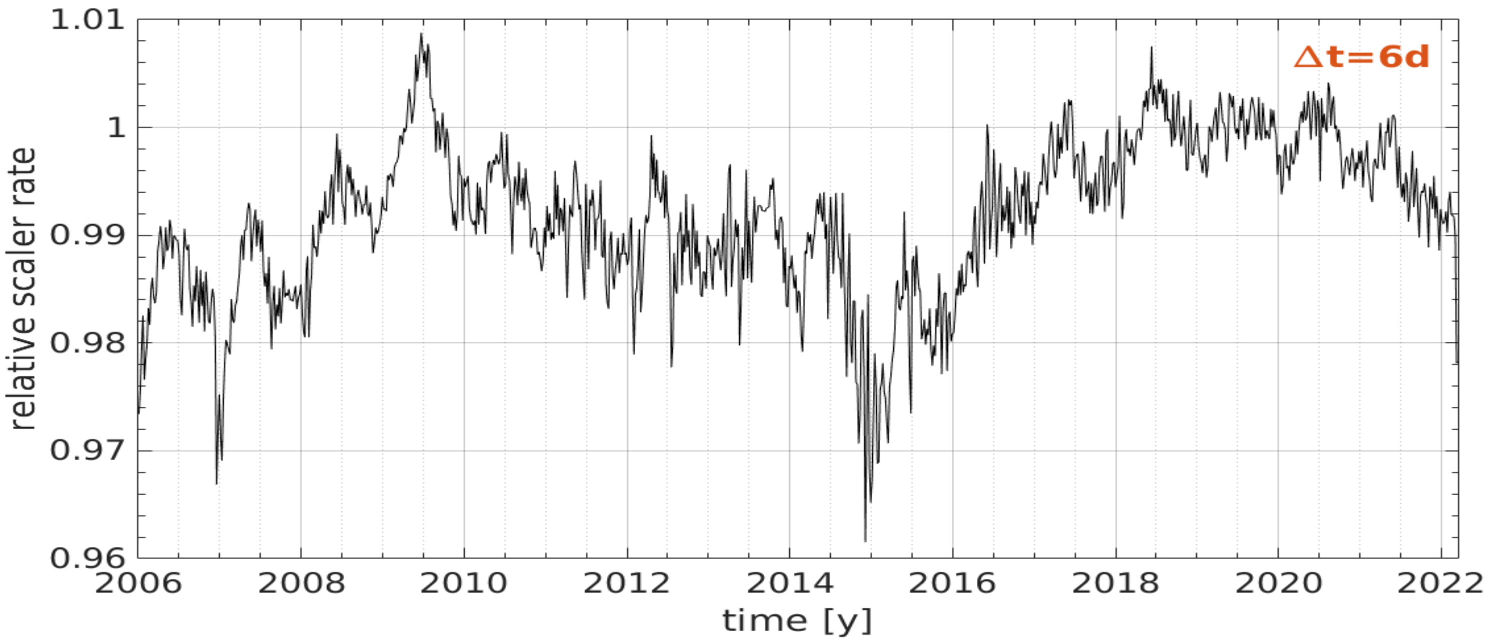


- **Covered period**: from January 1st, 2006, to March 21st, 2022 (≈ 16 y)
- Scaler data:
  1. stored every second from each detector
  2. corrected for pressure, lightning events and malfunctioning factors *(M. Schimassek, 2022)*
  3. scaled to a known reference value (the mean count rate for 2013) obtaining the **relative scaler rate r(t)**
  4. Gap-filling procedure based on an AR model
- **Time resolution**: depending on the timescale of interest, different time resolutions were used (6 days, 2 days, 1 hour and 15 minutes).

# SPECTRAL ANALYSIS

Spectral methods:

- **Singular Spectrum Analysis and Monte Carlo test (MC-SSA)**
- **Continuous Wavelet Transform (CWT)**

Monte-Carlo approach: different null-hypothesis

Final spectrum ➡ statistically significant spectral components (99% c.l.)

**Last (not rejectable) null-hypothesis:** AR(1) + RCs 11 y, 1 y, 9 months, 6 months, 28 d, 20 d, 14 d

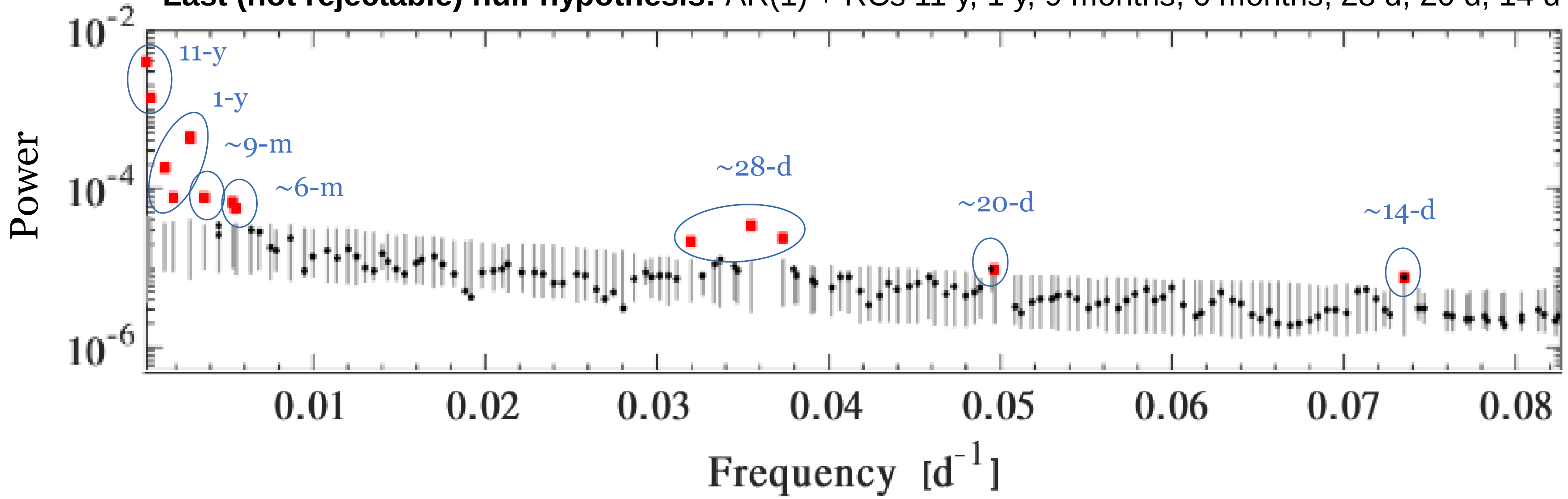


$\Delta t$=6d

M=150

# Significant recontructed components

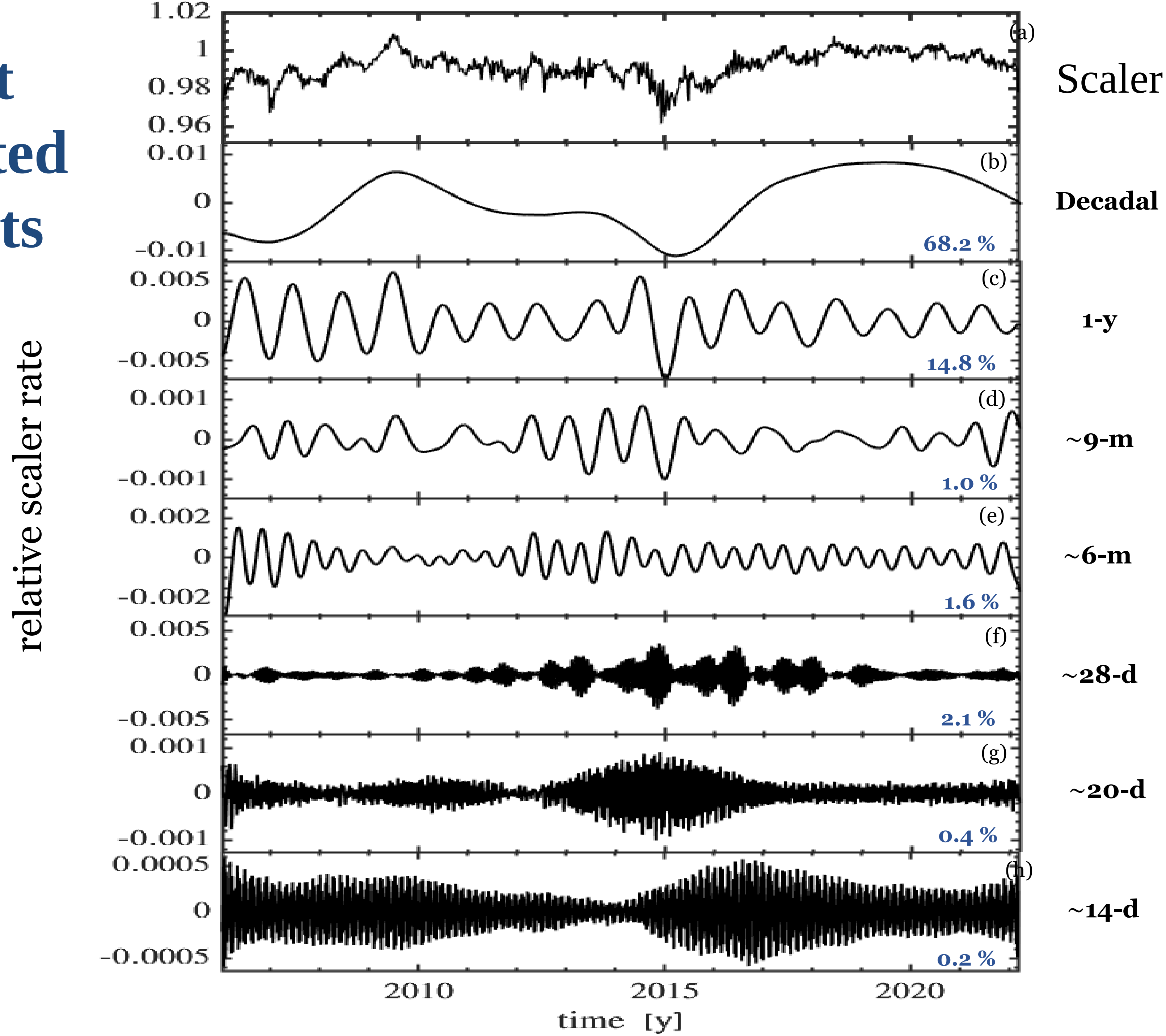


% of the total variance

Amplitude and phase modulations

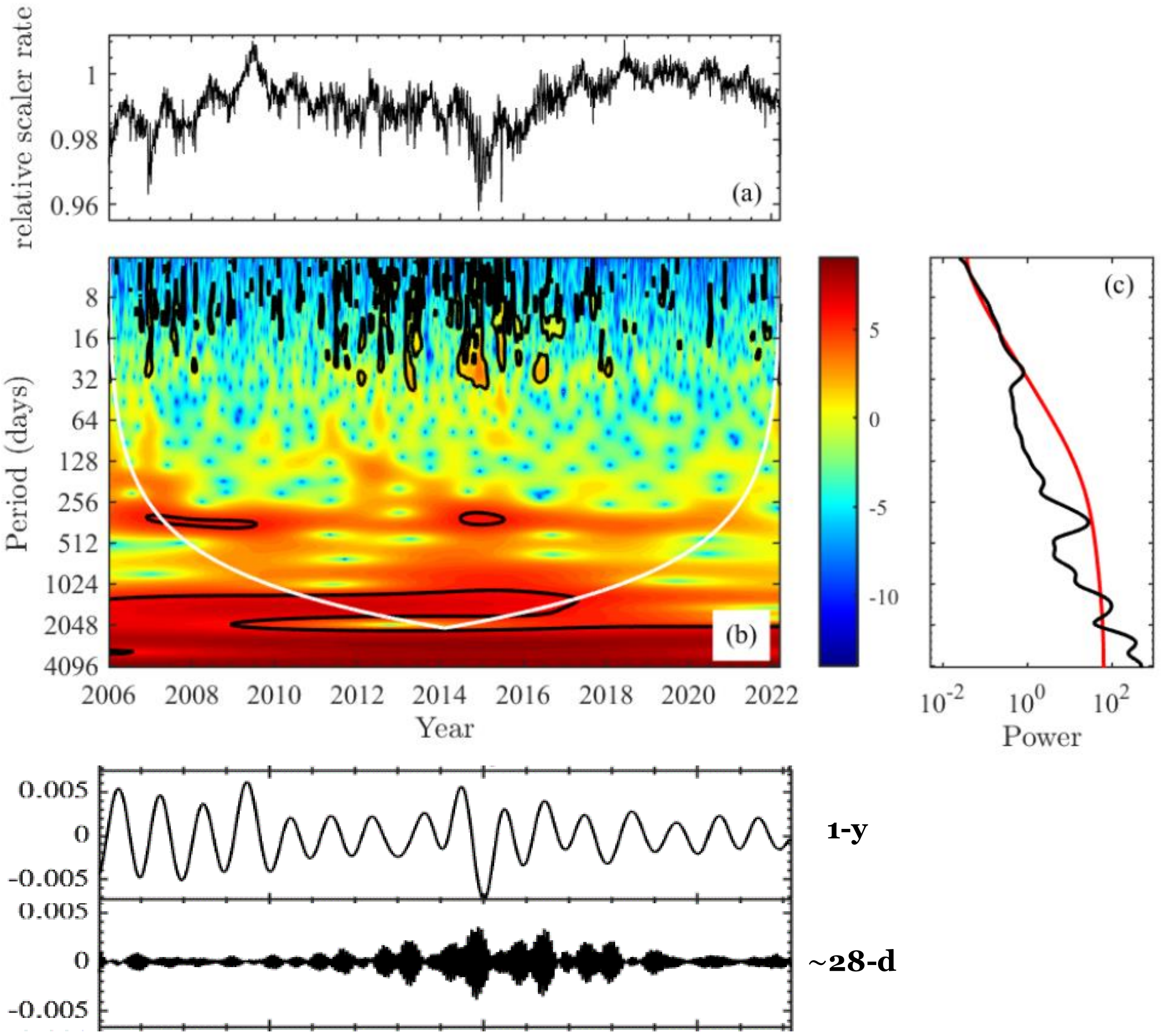
relative scaler rate
1
0.98
0.96
(a)
8
16
32
64
128
256
512
1024
2048
4096
Period (days)
(b)
2006
2008
2010
2012
2014
2016
2018
2020
2022
Year
5
0
-5
-10
(c)
Power
0.005
0
-0.005
1-y
~28-d

SSA

# SCALERS AND SUNSPOT AREAS

- **Very similar spectral content; low noise in scalers!**

- **~6-months**: Rieger-type periodicity with ~186-d period:
  - detected in various indicators of solar magnetic activity (X-ray flares, 10.7 cm radio flux)

**~9-months**: detected in several solar activity indices (10.7 cm radio flux, coronal index)

**The physical origin of these solar periodicities is not entirely clear**

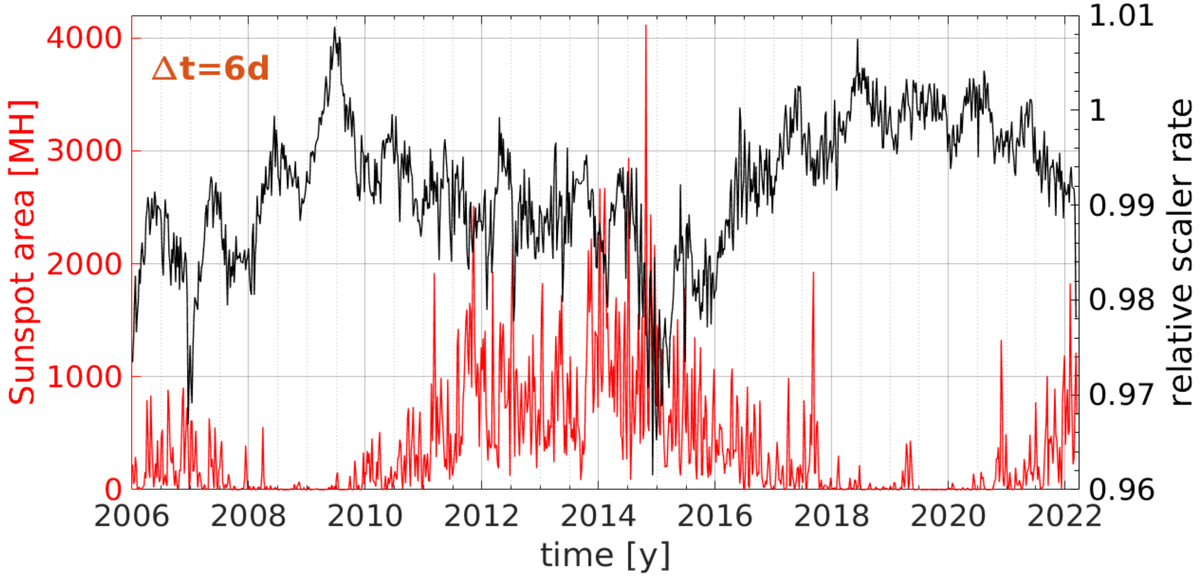


| SSA SIGNIFICANT COMPONENT (99% c.l.) | | |
|---|---|---|
| | SCALERS | TOTAL SUNSPOT AREA |
| Period | Variance [%] | |
| 11 y | 68.2 | 53.7 |
| 1.2 y | - | - |
| 1 y | 14.8 | - |
| ~9 months | 1.0 | 4.0 |
| ~6 months | 1.6 | 2.4 |
| ~28 d | 2.1 | 7.0 |
| 20 d | 0.4 | 3.0 |
| ~14 d | 0.2 | - |

| | | |
|---|---|---|
| SIGNAL | ~88% | ~70% |
| NOISE | ~12% | ~30% |

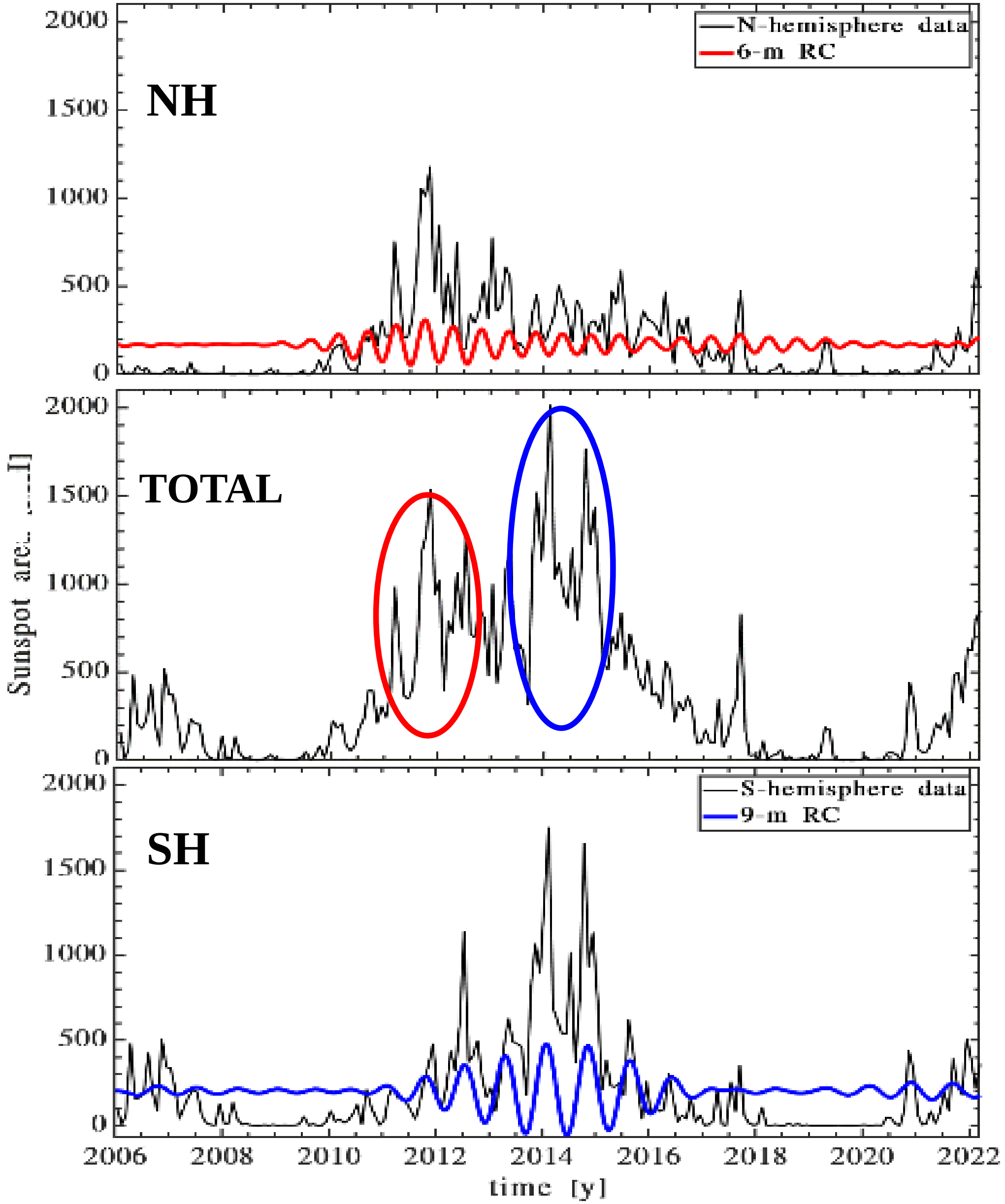


*Archive: United States Air Force (USAF) Solar Observing Optical Network (SOON)*

The total sunspot-areas series shows 2 peaks:

**~2012 peak** **~2014-2015 peak**

The analysis of the hemispheric sunspot-areas series shows that

**the 6-months oscillation comes from the Northern hemisphere**

**the 9-months oscillation comes from the Southern hemisphere**

| SSA SIGNIFICANT COMPONENT (99% c.l.) | | | | |
|---|---|---|---|---|
| | SCALERS | TOTAL SUNSPOT AREA | SUNSPOT AREA NORTH | SUNSPOT AREA SOUTH |
| Period | Variance [%] | | | |
| 11 y | 68.2 | 53.7 | 37.8 | 40.7 |
| 1.2 y | - | - | - | - |
| 1 y | 14.8 | - | - | - |
| ~9 months | 1.0 | 4.0 | - | 6.2 |
| ~6 months | 1.6 | 2.4 | 3.4* | - |
| ~4 months | - | - | - | - |
| ~28 d | 2.1 | 7.0 | 8.1 | 12.0 |
| 20 d | 0.4 | 3.0 | 3.5 | - |
| ~14 d | 0.2 | - | - | - |
| SIGNAL | ~88% | ~70% | ~53% | ~59% |
| NOISE | ~12% | ~30% | ~47% | ~41% |

# RESULTS CONFIRMED BY THE CWT METHOD



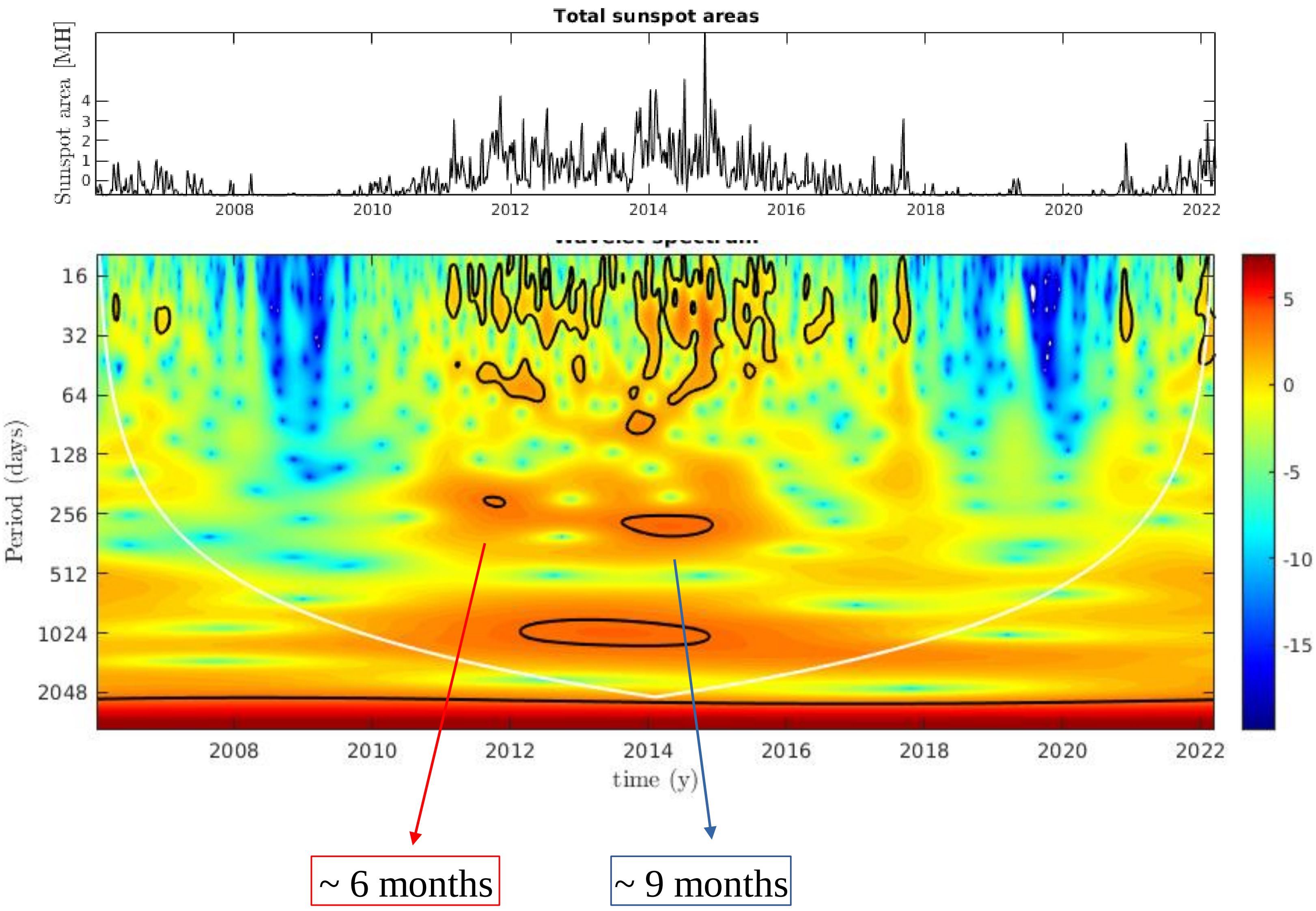


The CWT spectral analysis of the total sunspot areas confirms

- the presence of the 6 and 9 months modulations
- maximum amplitudes correspond to the first (2012) and second peak (2015) respectively

# SCALERS AND SUNSPOT NUMBER: decadal cycle

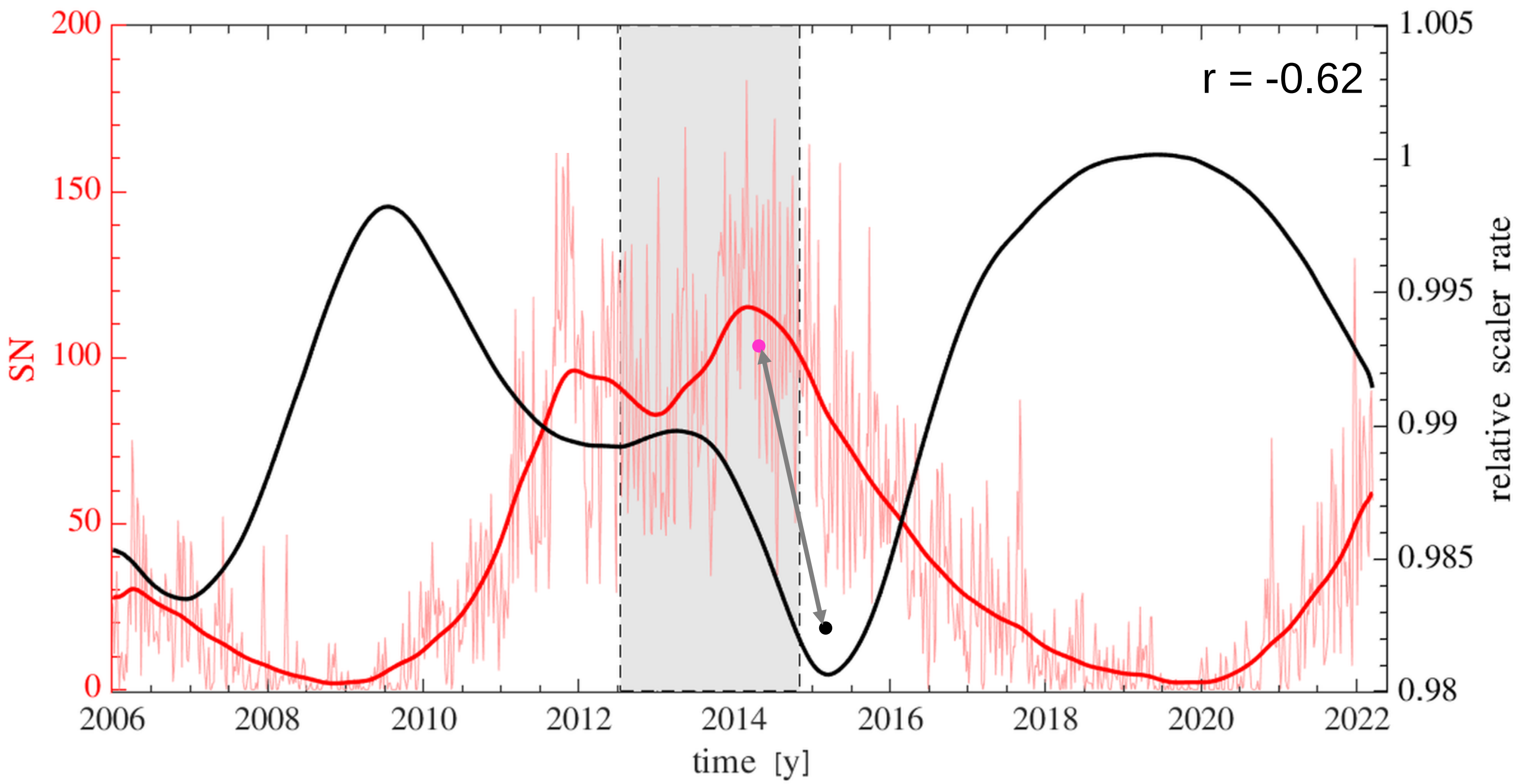


General agreement

Anticorrelation

Scalers delay of ~1-year in the period 2014-2015

Draft version February 3, 2025
Typeset using LaTeX default style in AASTeX631

ApJ (under review)

# Scaler rates from the Pierre Auger Observatory: a new proxy of solar activity

The Pierre Auger Collaboration,[1] I. Bizzarri,[2] C. Dionese,[2] and S. Mancuso[3]

[1]Observatorio Pierre Auger, Av. San Martín Norte 304, 5613 Malargüe, Argentina
[2]Dipartimento di Fisica, Università degli Studi di Torino, Via Pietro Giuria 1, Torino, Italy
[3]INAF, Osservatorio Astrofisico di Torino, via Osservatorio 20, Pino Torinese 10025, Italy

## ABSTRACT

The modulation of low-energy galactic cosmic rays reflects interplanetary magnetic field variations and can provide useful information on solar activity. An array of ground-surface detectors can reveal the secondary particles, which originate from the interaction of cosmic rays with the atmosphere. In this work, we present the investigation of the low-threshold rate (scaler) time series recorded in 16 years of operation by the Pierre Auger Observatory surface detectors in Malargüe, Argentina. Through an advanced spectral analysis, we detected highly statistically significant variations in the time series with periods ranging from the decadal to the daily scale. We investigate their origin, revealing a direct connection with solar variability. Thanks to their intrinsic very low noise level, the Auger scalers allow a thorough and detailed investigation of the galactic cosmic ray flux variations in the heliosphere at different timescales and can, therefore, be considered a new proxy of solar variability.

*Keywords:* ISM:cosmic rays – Sun:sunspots – Methods: data analysis

## 1. INTRODUCTION

During their propagation through the heliosphere, Galactic Cosmic Rays (GCRs) interact with the solar wind and the heliospheric magnetic field, which modify their energy spectra. Changes in the interplanetary medium related to variations in the Sun's activity and to solar transient events thus determine the magnetic deflection of the trajectories of GCR particles, modifying the flux of the GCRs reaching the Earth's atmosphere.

The process through which GCR particles interact with magnetic irregularities in the solar wind can be described as a diffusion combined with convection and adiabatic energy losses (Parker 1965). In particular, during the minimum phase of solar activity, when the Sun is quiet, GCRs have a maximum intensity at Earth, and vice versa during solar maximum conditions, so solar activity effectively modulates periodically the GCR flux with the same solar decadal cycle. Apart from this long-term modulation associated with the solar cycle, short-term variations of the flux of GCRs are also produced by the perturbed interplanetary condition near the Earth, such as interplanetary coronal mass ejections (ICMEs) (e.g., Richardson & Cane 2010) or stream interaction regions (SIRs) (e.g., Richardson 2018). These temporal depressions in the GCR flux, generally known as Forbush decreases (Forbush 1937), are a consequence of changes on the GCRs transport plasma properties. While ICMEs are manifestations of solar eruptions, SIRs arise

# Solar magnetic field (paper in preparation)

- Heliospheric magnetic field intensity (|B|) and radial component ($B_r$) from the magnetic spectrometer on board the Advanced Composition Explorer (ACE).

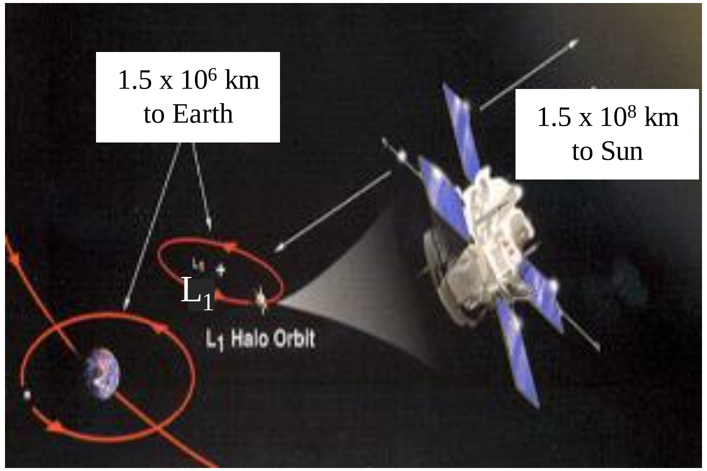


- Orbit around $L_1$ Lagrangian point

*image credit: NASA, Caltech*

- Coronal magnetic field at 2.5 $R_\odot$ in correspondence of the solar equator ($B_{2.5\ R\odot}$) extrapolated from the photospheric magnetic field data, acquired by the solar magnetometer of the Wilcox Solar Observatory (WSO) at the Stanford University, by using a potential field model. Indication of the warping of Heliospheric Current Sheet (HCS).

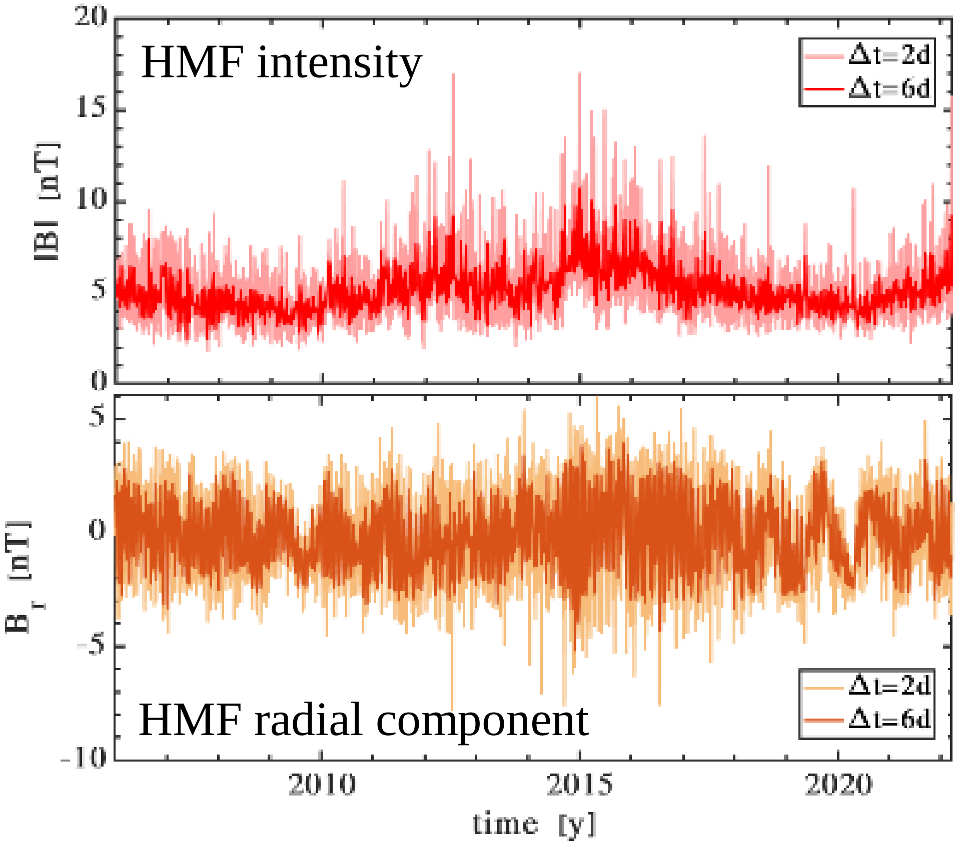


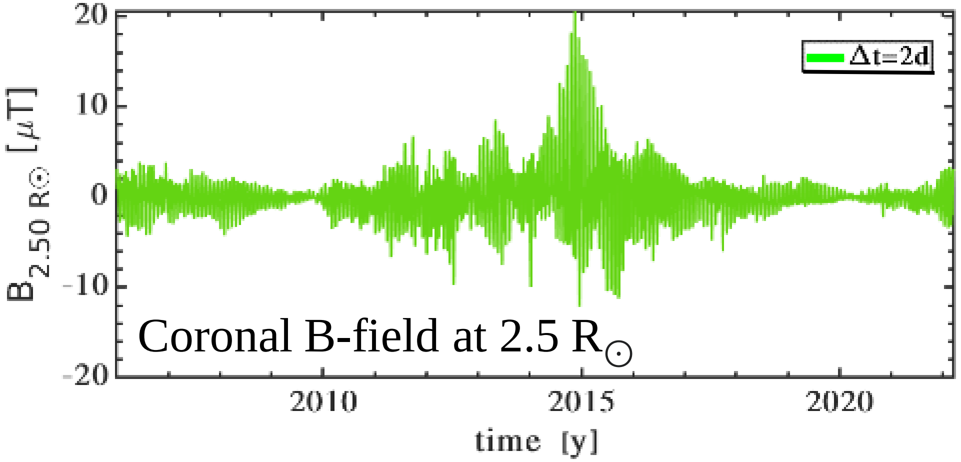

# SCALERS AND HMF INTENSITY |B| COMPARISON

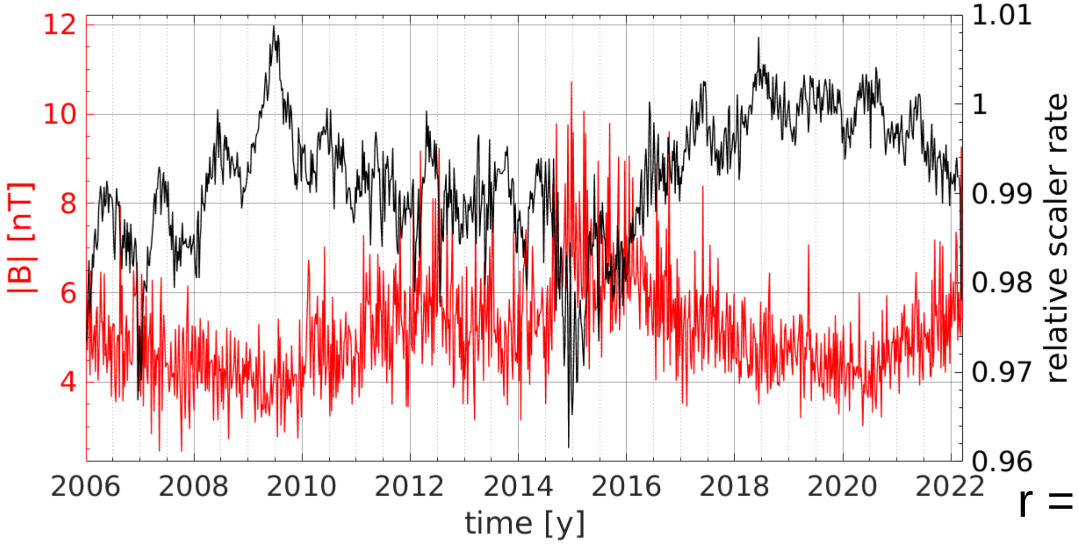


r = -0.43

Scaler data shows a general agreement with the HMF intensity

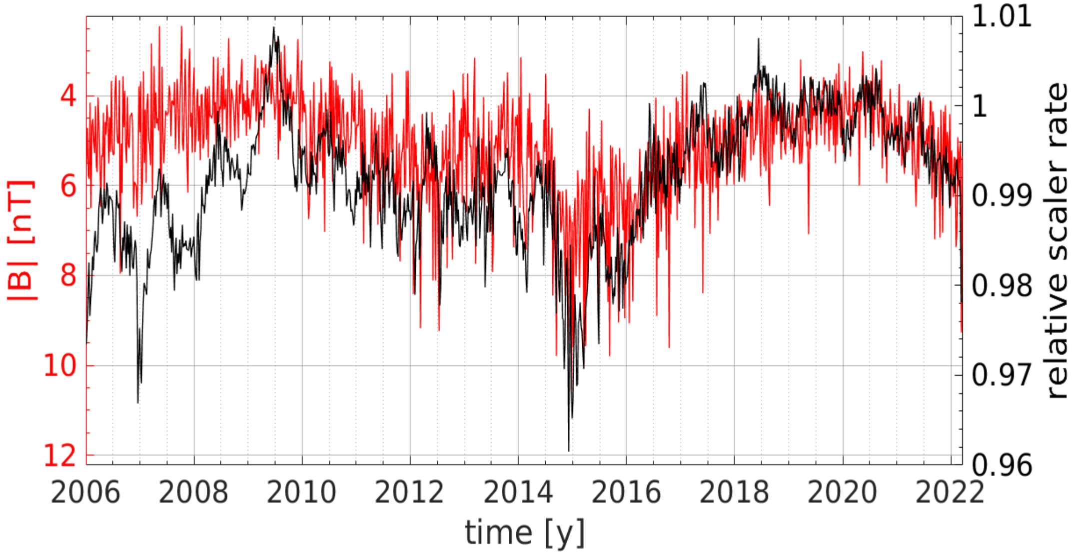


**high HMF intensity ➡ low scaler rate**

# SCALERS AND HMF INTENSITY |B| COMPARISON

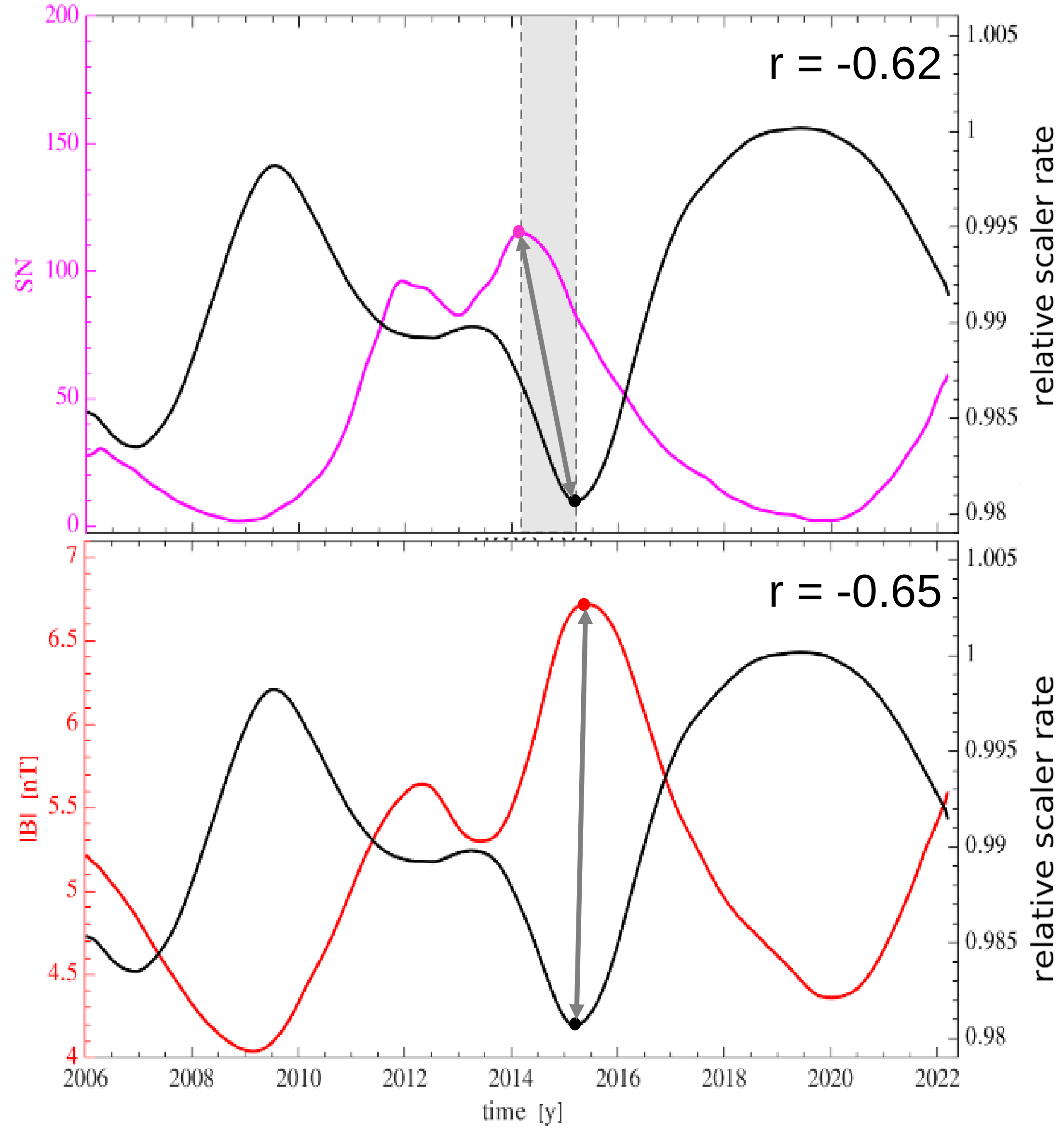


**SCALERS AND SUNSPOT NUMBER**

**SCALERS AND HMF INTENSITY**

Using HMF intensity as solar activity proxy
the high delay disappears

MF is a better marker for solar
activity than sunpot number

# SPECTRAL COMPARISON
## Singular Spectrum Analysis (SSA): significant (99% c.l.) components

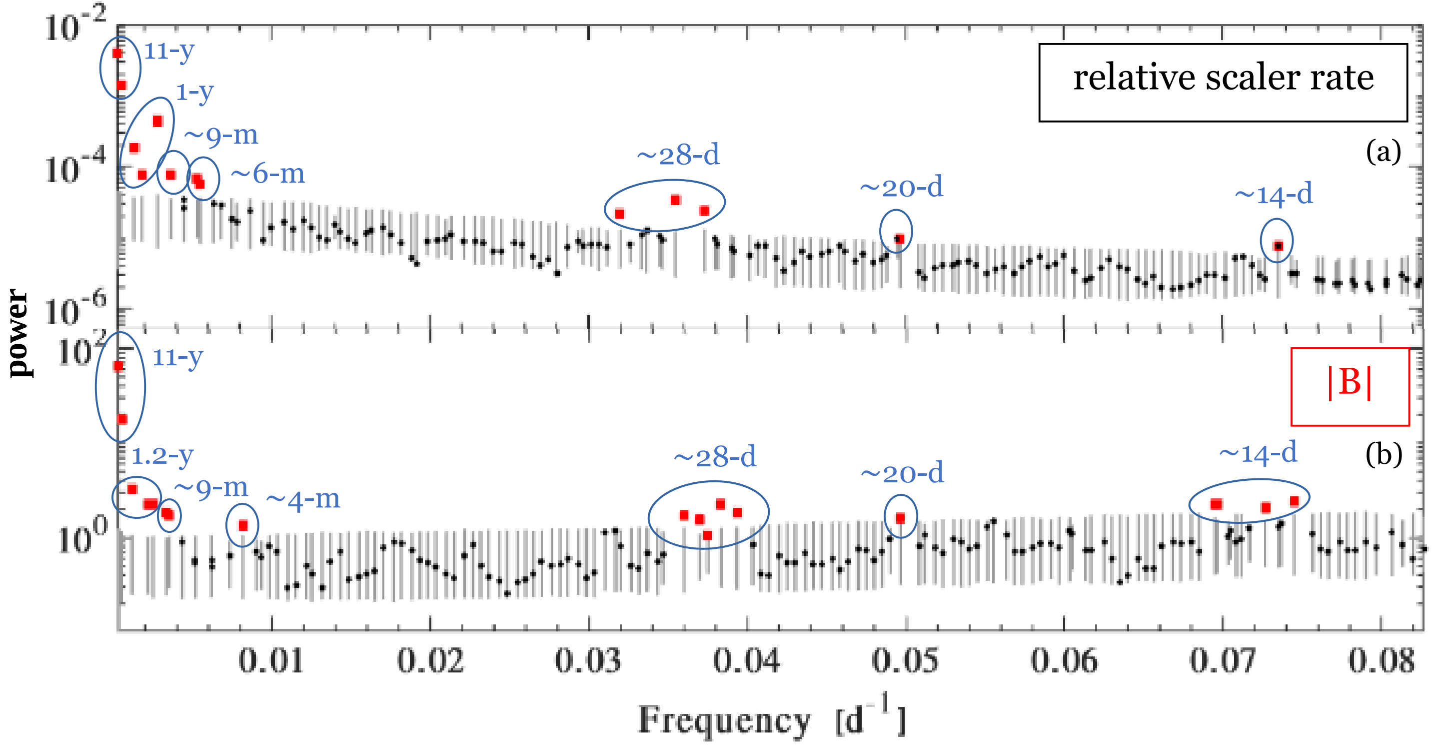


SSA SIGNIFICANT COMPONENTS 99% c.l. – Δt = 6d

| | SCALERS | \|B\| |
|---|---|---|
| Period | Variance [%] | |
| Trend (~11 y) | 68.2 | 37.9 |
| 1.2-y | - | 3.6 |
| 1-y | 14.8 | - |
| ~9-m | 1.0 | 1.7 |
| ~6-m | 1.6 | - |
| ~4-m | - | 1.3 |
| ~28-d | 2.1 | 6.9 |
| ~20-d | 0.4 | 1.5 |
| ~14-d | 0.2 | 6.3 |

| | | |
|---|---|---|
| SIGNAL | ~88% | ~59% |
| NOISE | ~12% | ~41% |

**Low noise level in the scalers!**

- **Impressive similarity of the spectra**: almost all the |B| components are recorded by scaler data
- Components related to the Sun
- 1.2-y component, known to characterize solar activity, not revealed in the scalers due to the high power of the very close annual peak

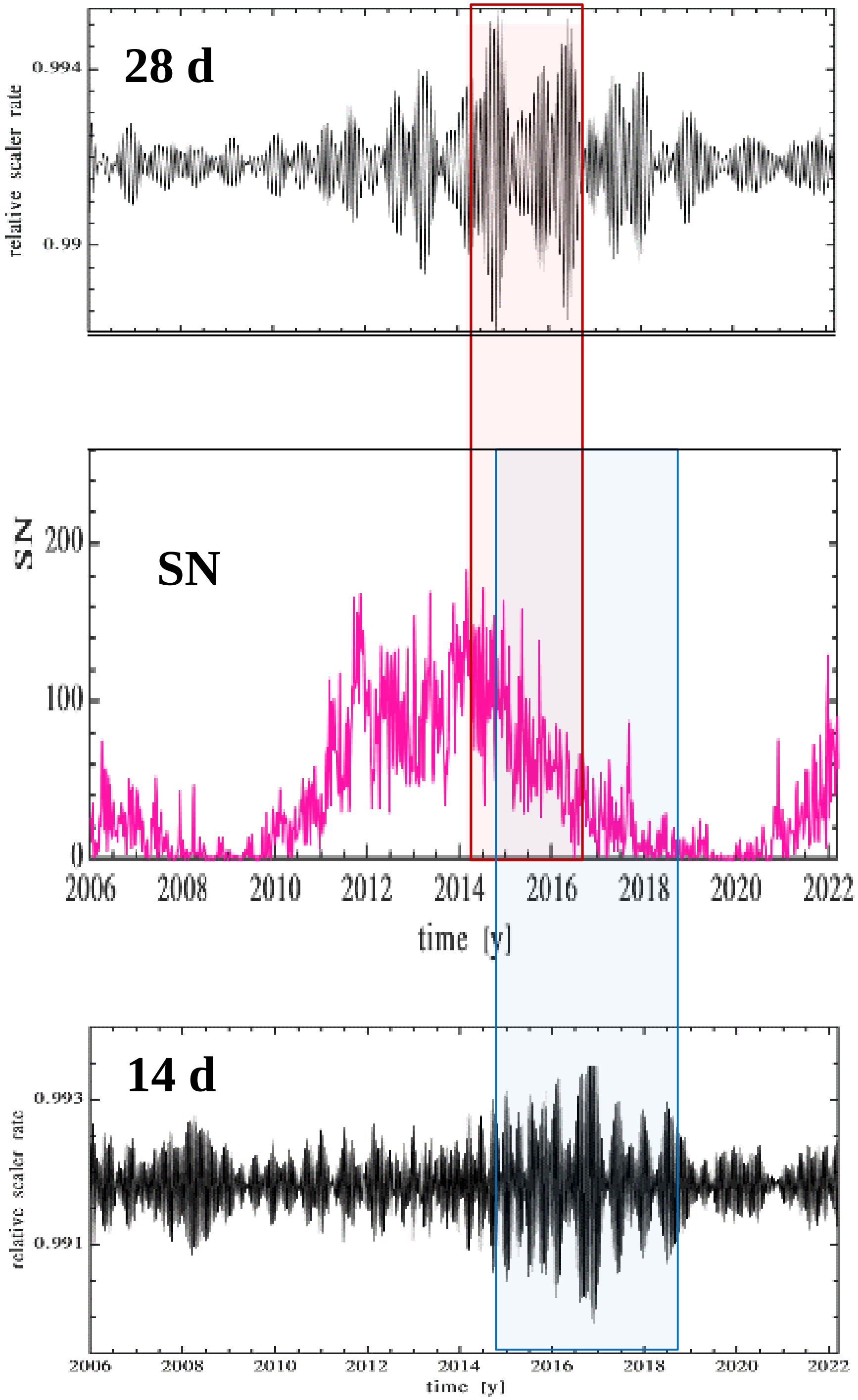


# 28- and 14-d components reconstructed by SSA

Scalers shows that the **28-d and 14-d cycles** have higher variability in the declining phase of the solar cycle (maximum of the HMF intensity!) → a period characterized by more robust long-lived solar active regions (more intense solar flares and CMEs)

*ICRC2025*

# 28- and 14-d components reconstructed by SSA

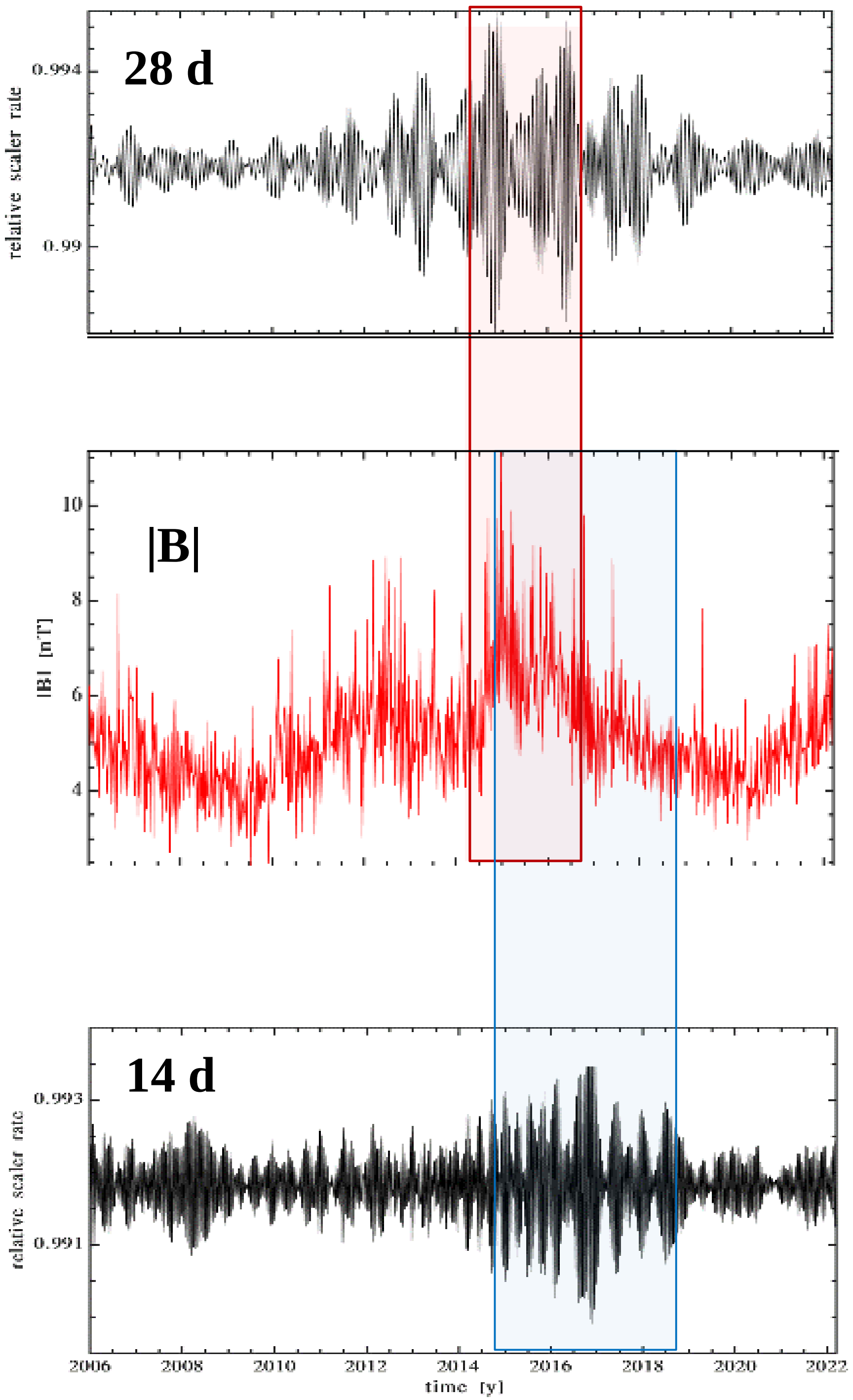


Scalers shows that the **28-d and 14-d cycles** have higher variability in the declining phase of the solar cycle (maximum of the HMF intensity!) → a period characterized by more robust long-lived solar active regions (more intense solar flares and CMEs)

*ICRC2025*

# FUTURE PLANS and WORK IN PROGRESS

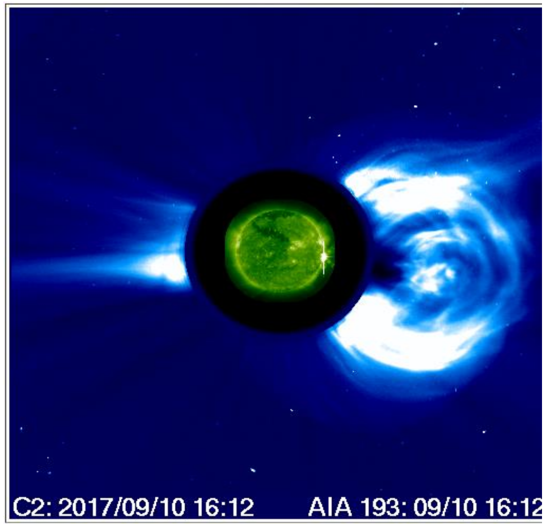


Sensitivity of scalers to **sudden solar variations**
(analysis of high resolution (1 h or less) scalers series):

- **Identification of Forbush decreases**
- Is there an inprint in the scalers of **Solar Energetic Particles** generated impulsively by powerful solar flares or gradually by coronal shocks?
- Correlation between the detected Forbush events and **Interplanetary Coronal Mass Ejections** to **identify the origin of the Forbush decreases**
- Comparison between **scalers and neutron monitors** at similar latitudes

We need high-resolution scaler series!

# Identification of Forbush decreases (in progress)

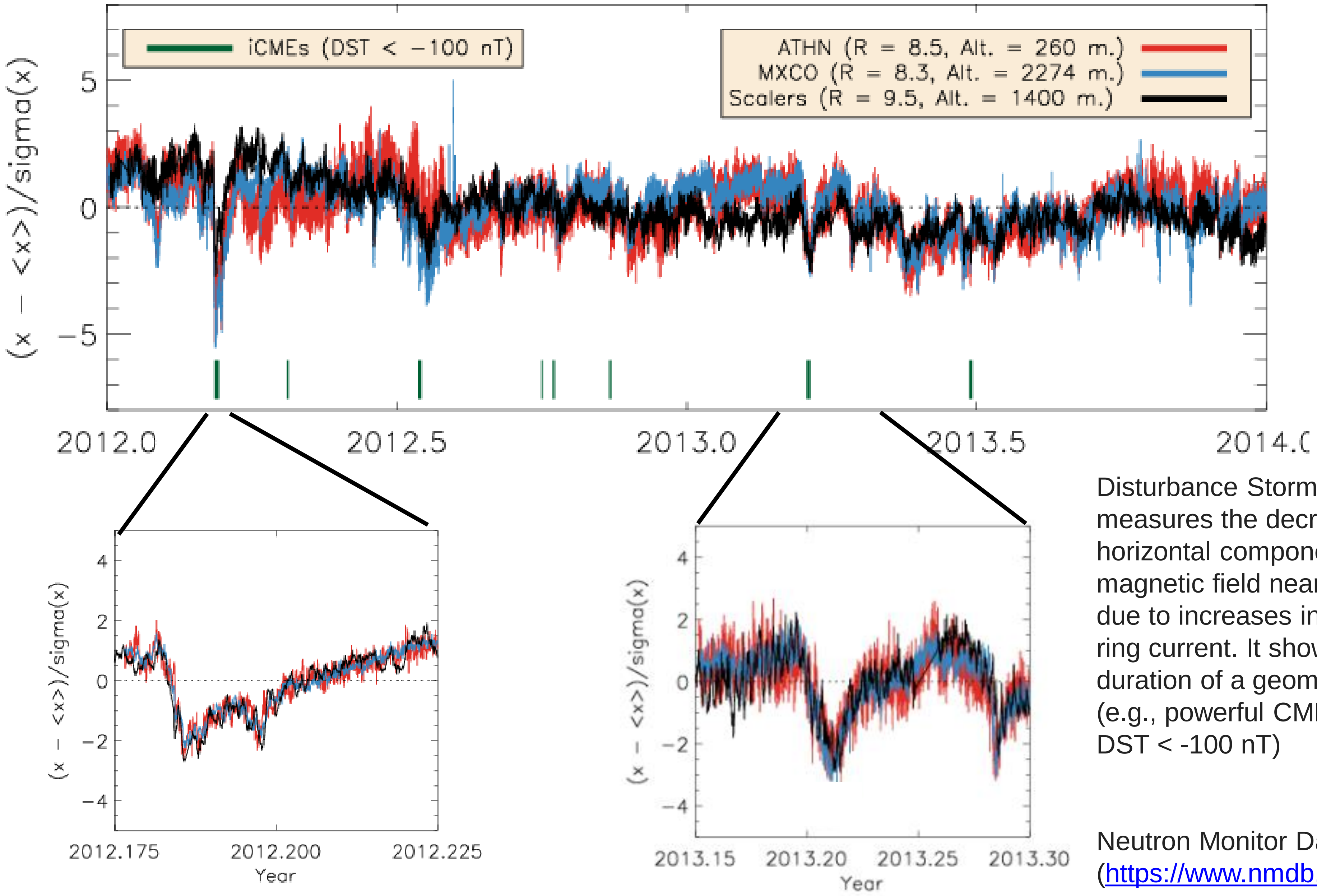


Disturbance Storm Time (DST) index: measures the decrease in the horizontal component of the Earth's magnetic field near the magnetic equator due to increases in the magnetospheric ring current. It shows the strength and duration of a geomagnetic storm (e.g., powerful CME --> strong storm --> DST < -100 nT)

Neutron Monitor Database ([https://www.nmdb.eu](https://www.nmdb.eu))

# CONCLUSIONS

We have spectrally characterized the scaler series, identifying its strong relationship with solar activity

Great advantage: <u>intrinsic</u> very low noise level, allowing detailed investigations of the GCR flux variations in the heliosphere

→ good opportunity for interesting studies at high resolution

***Thank you for your attention!***

# BACKUP

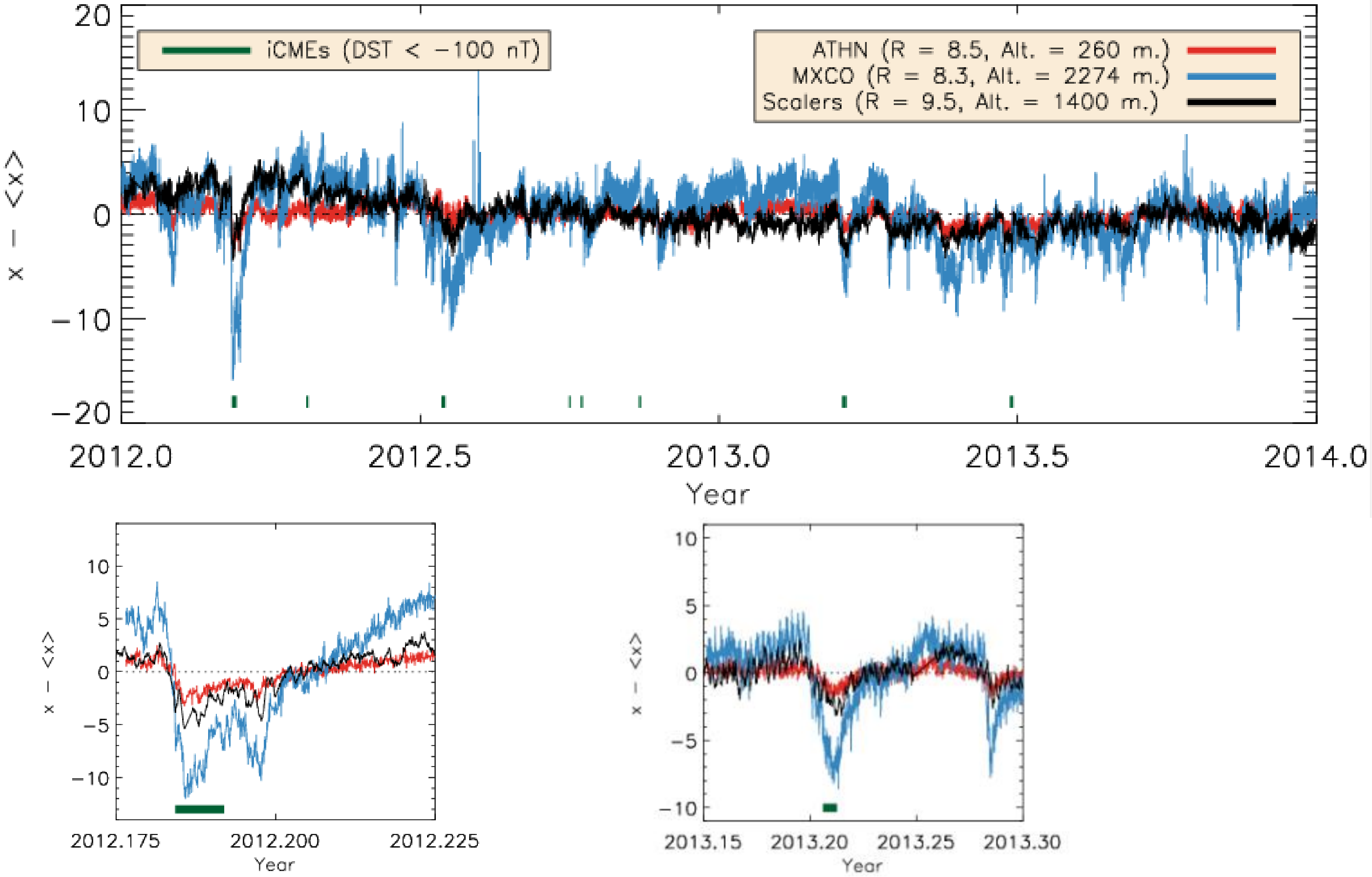

iCMEs (DST < −100 nT)
ATHN (R = 8.5, Alt. = 260 m.)
MXCO (R = 8.3, Alt. = 2274 m.)
Scalers (R = 9.5, Alt. = 1400 m.)
x − <x>
Year
2012.0
2012.5
2013.0
2013.5
2014.0
2012.175
2012.200
2012.225
2013.15
2013.20
2013.25
2013.30

# SOLAR ACTIVITY AND COSMIC RAYS FLUX

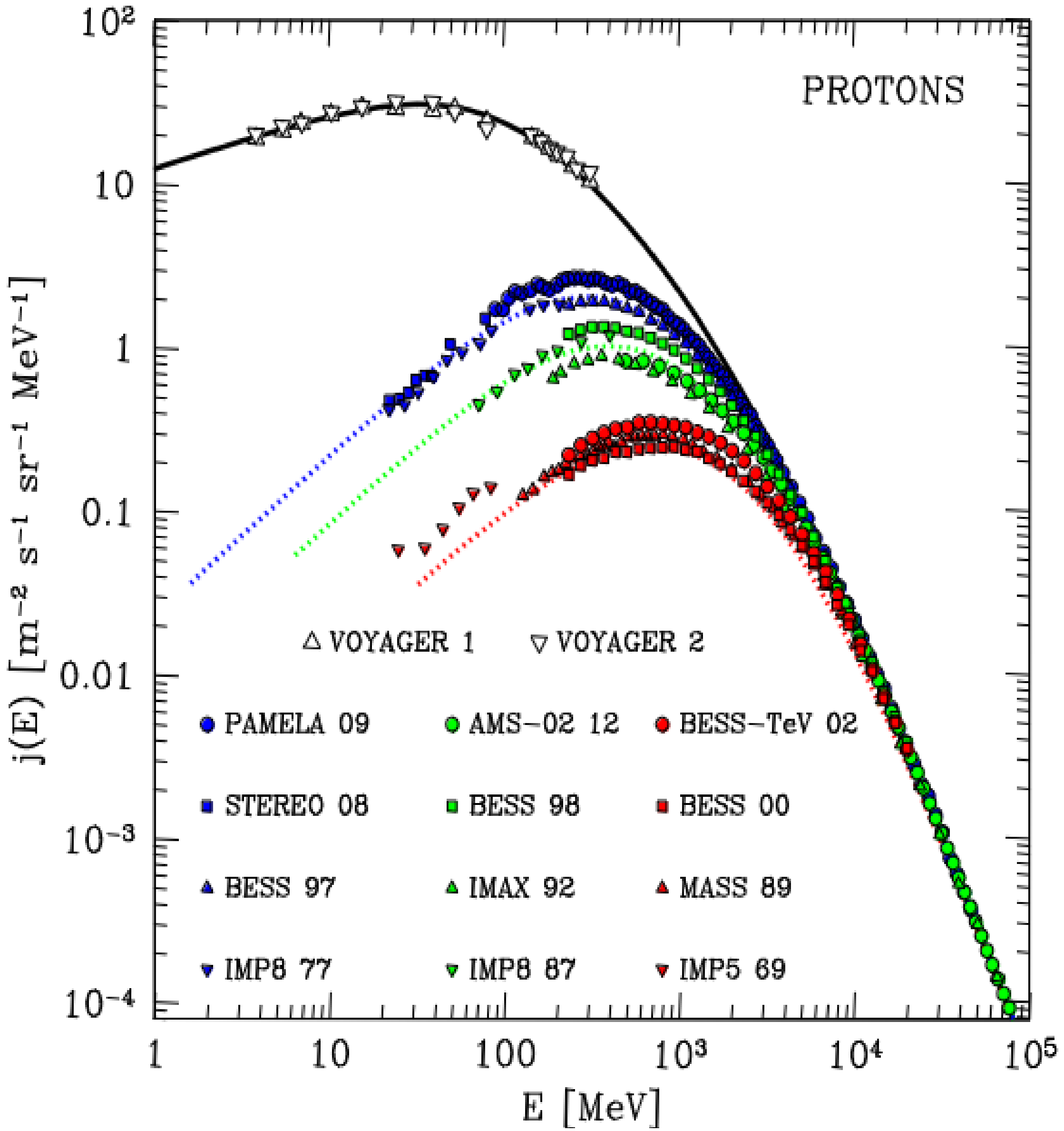


*Gabici, S. Low-energy cosmic rays: regulators of the dense interstellar medium. Astron Astrophys Rev 30, 4 (2022)*

- **Low energy cosmic rays** are modulated by solar activity through the influence of magnetic field and solar wind
- Modulation on decadal scale: blue and red spectra correspond to periods of minimum and maximum of solar activity
- Auger scaler rates: measurements of **low energy CRs** corresponding to a deposited energy range **[15-100] MeV** (primary CRs energies **from about 10 GeV to $10^3$ GeV**)

# THE DAILY DOUBLE PEAK (preliminary)

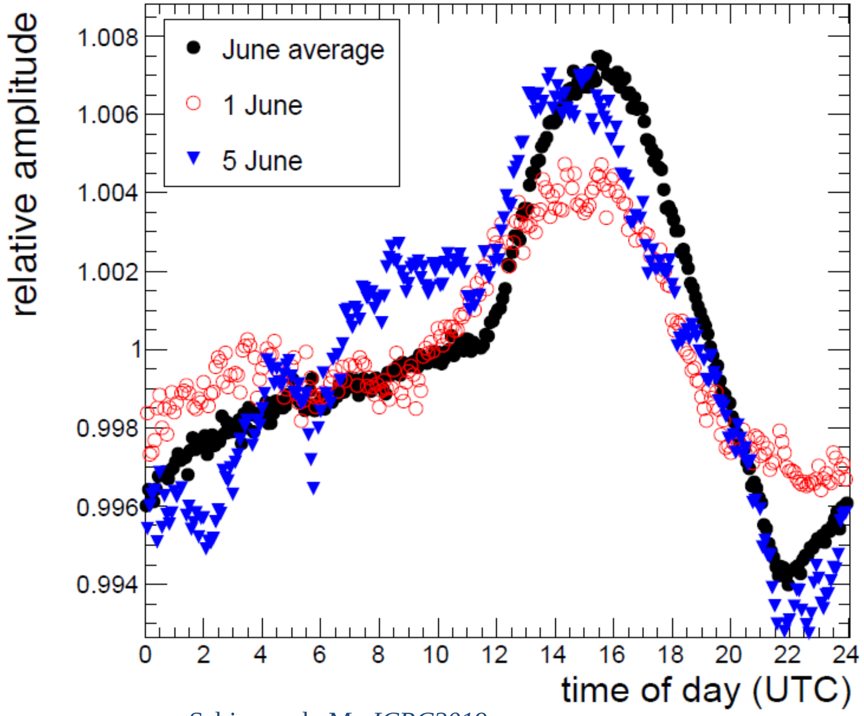


Schimassek, M., *ICRC2019*

Example for June 2018

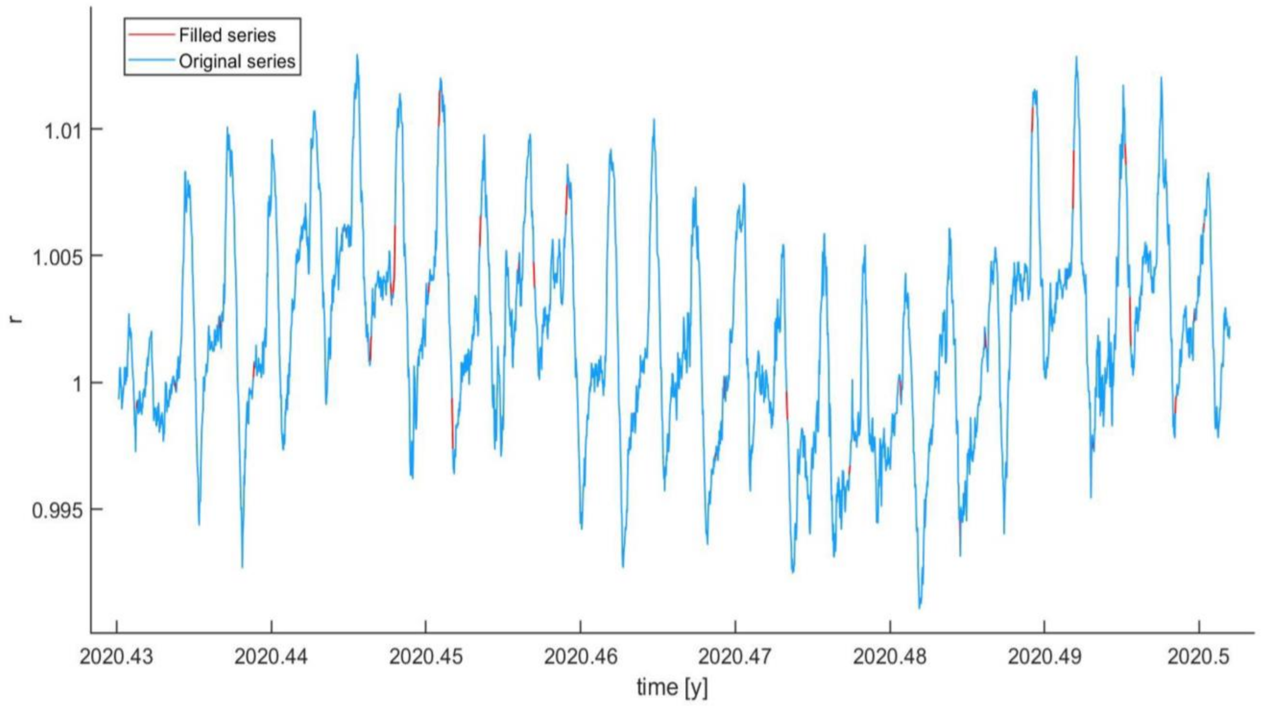


June 2020

Ts = 15 min

Series length = 2518 (~ 26 d)

The asymmetric shape is always present

**Asymmetric shape**

## Ts = 15min - 99% c.l. - M=500 (~5 d)

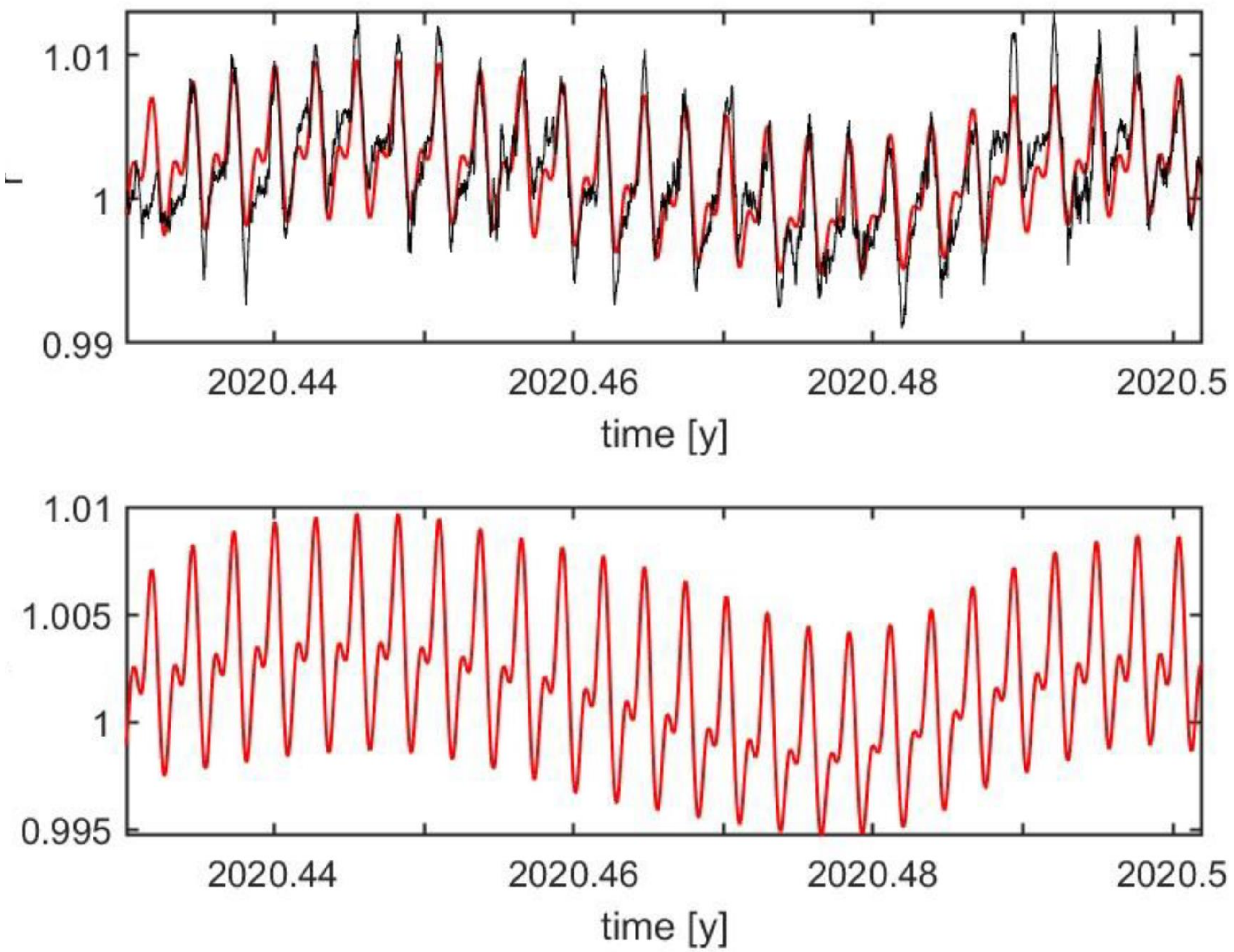


SSA: the asymmetric shape is due to the **presence of a 12 h cycle** superposed to the 24 h cycle

| SIGNIFICANT COMPONENT | | |
|---|---|---|
| Empirical Ortogonal Functions (EOFs) | Period | Variance [%] |
| 1-2-3-4-5 | 24 h + monthly + 12 h | 75.5 |

# The double peak is evident during periods of high and low solar activity

June 2010 (Solar minimum) June 2014 (Solar maximum) June 2020 (Solar minimum)

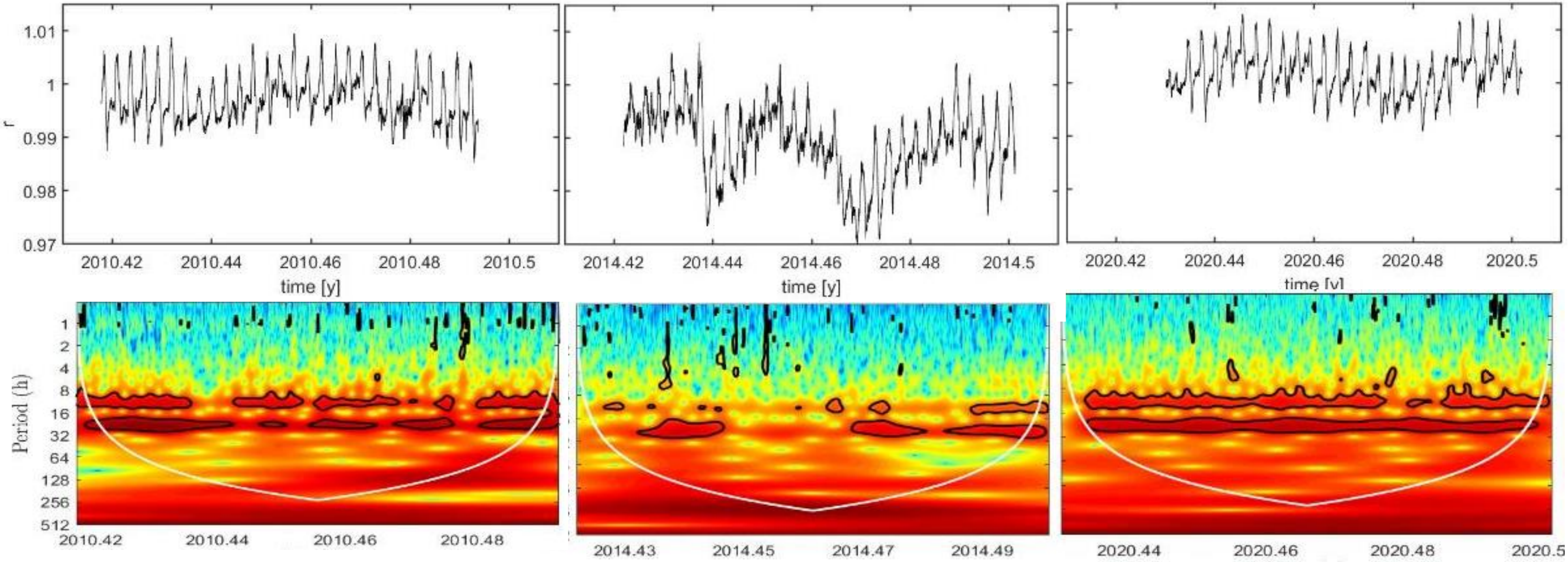

# WAVELET ANALYSIS

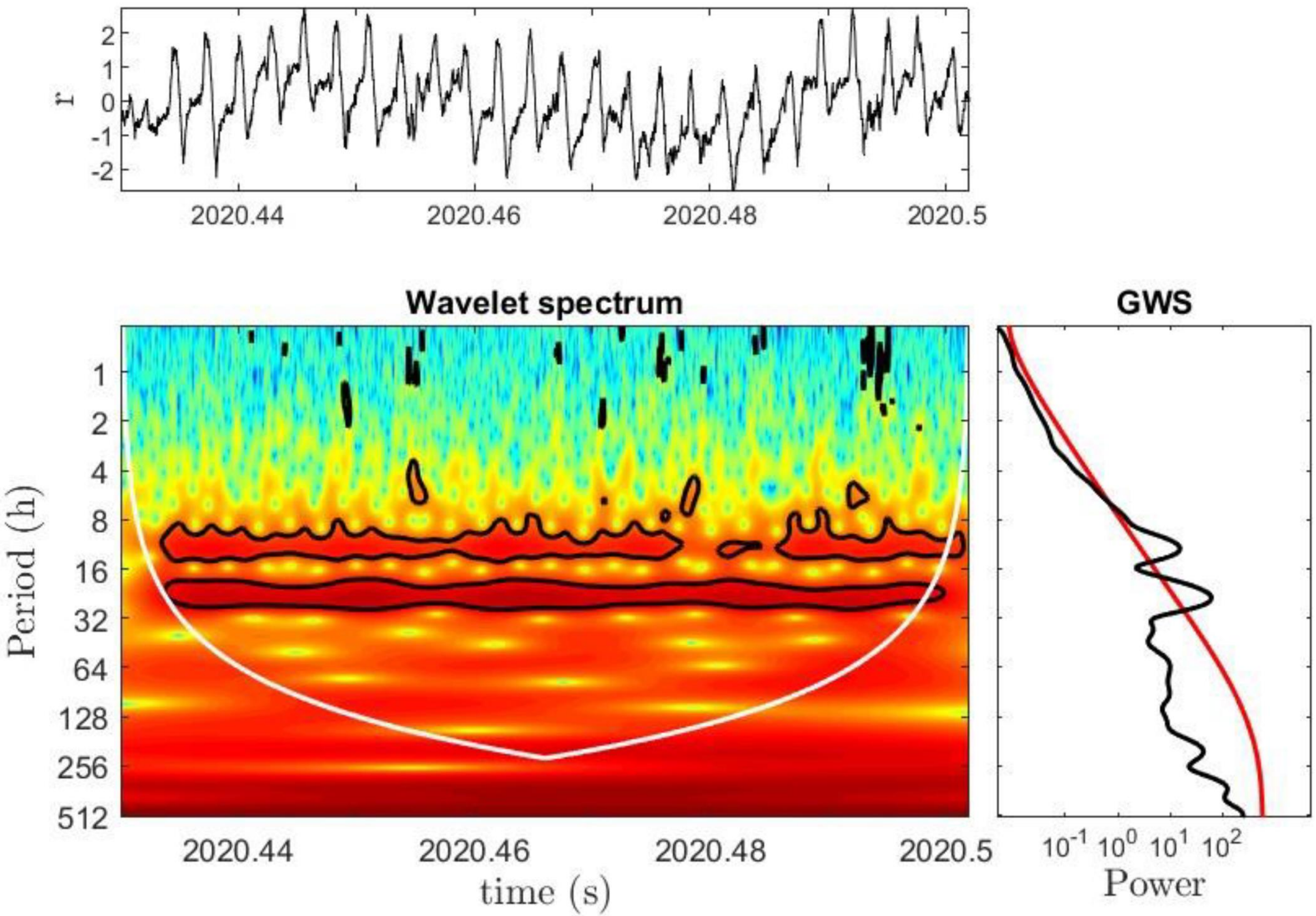

**Surface pressure shows a double peak!**

The daily double peak is everywhere

Is the scaler series well corrected for pressure?

The correction could be efficient on long-term but not on short-term (daily) scale

**Futher investigations are required**

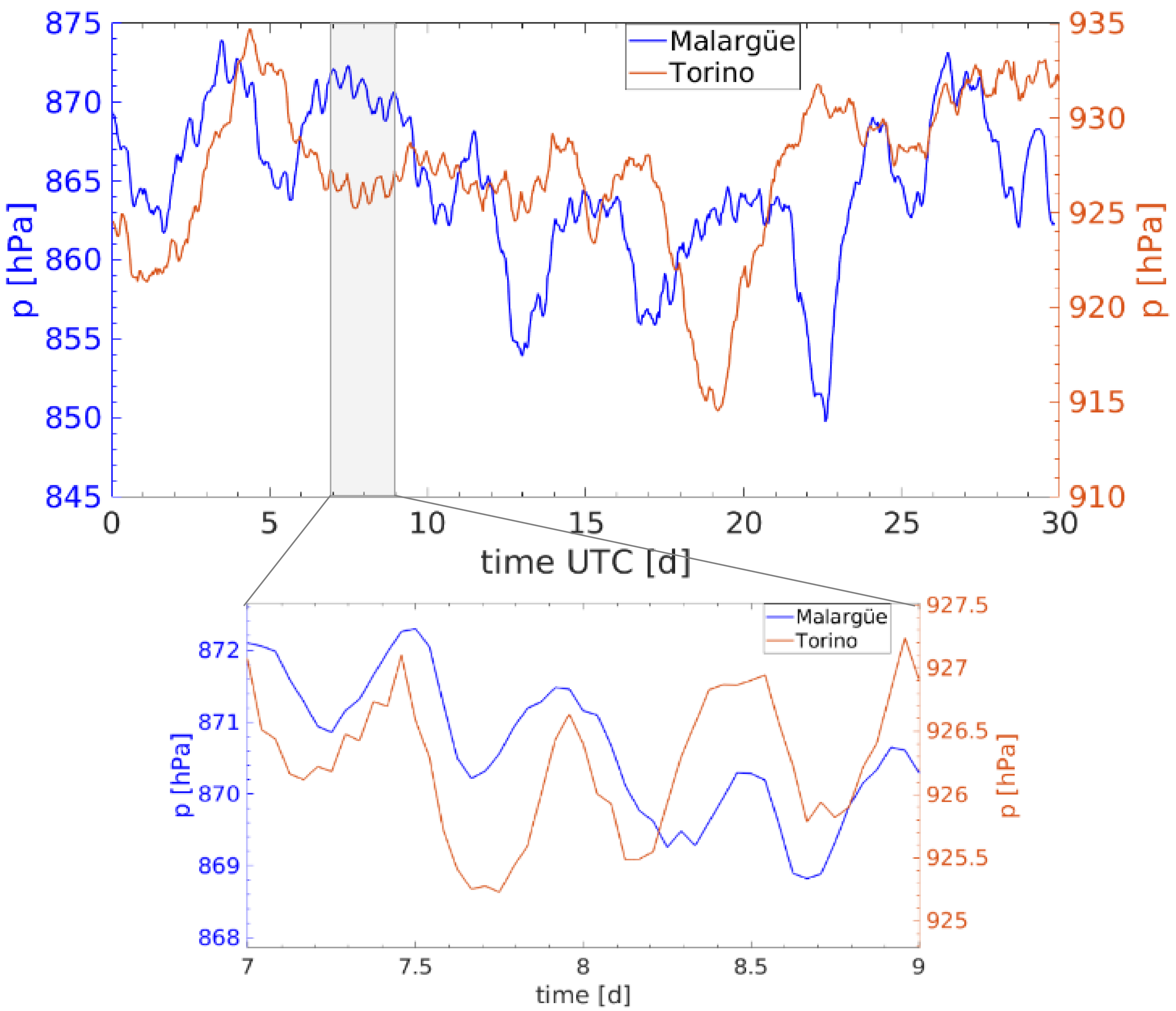

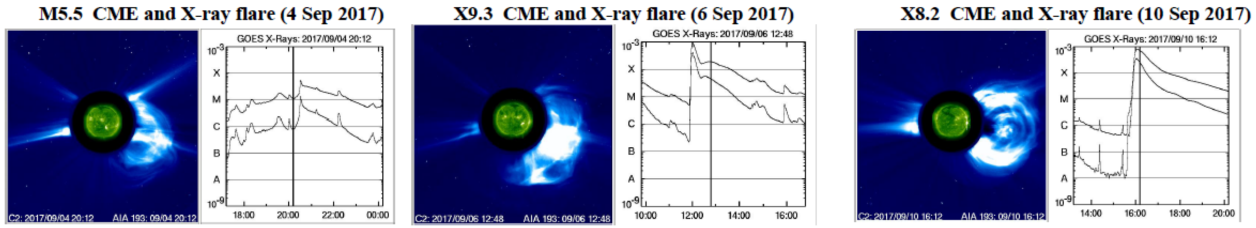


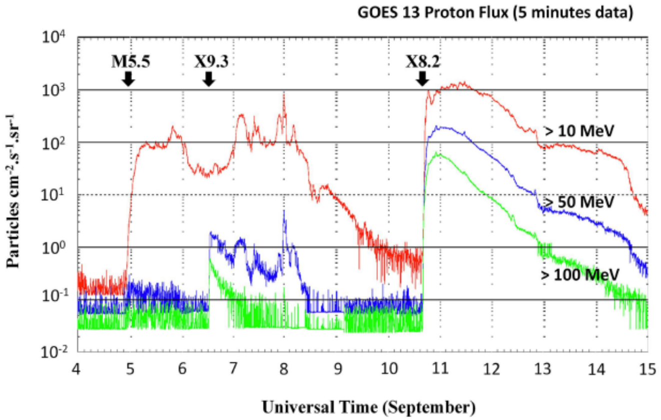


5-min-average integral proton fluxes measured from 4 to 15 Sep 2017 by GOES satellite for 3 energy thresholds.

Vertical arrows indicate the timing of the above 3 CME/flare events (from Hubert et al. 2019)

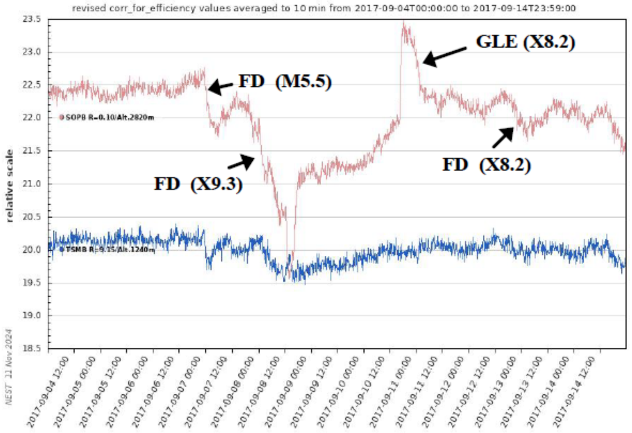


Count rates from 4 to 15 Sep 2017 for 2 NM stations:

- SOPB (South Pole, Antarctica, Cutoff = 0.10 GV)
- TSMB (Tsumeb, Namibia, Cutoff = 9.15 GV).

3 FDs (linked to the M5.5, X9.3, and X8.2 flares) are visible in both NM stations but only the GLE due to the X8.2 flare is clearly visible in the SOPB data due to the low rigidity cutoff of this station.

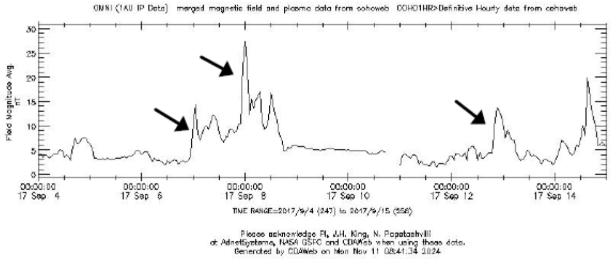

Average interplanetary magnetic field <B> at 1 AU from 4 to 15 Sep 2017: the 3 FDs (M5.5, X9.3, and X8.2 flares) match the sudden increases in <B>.

# THE GAP-FILLING PROCEDURE

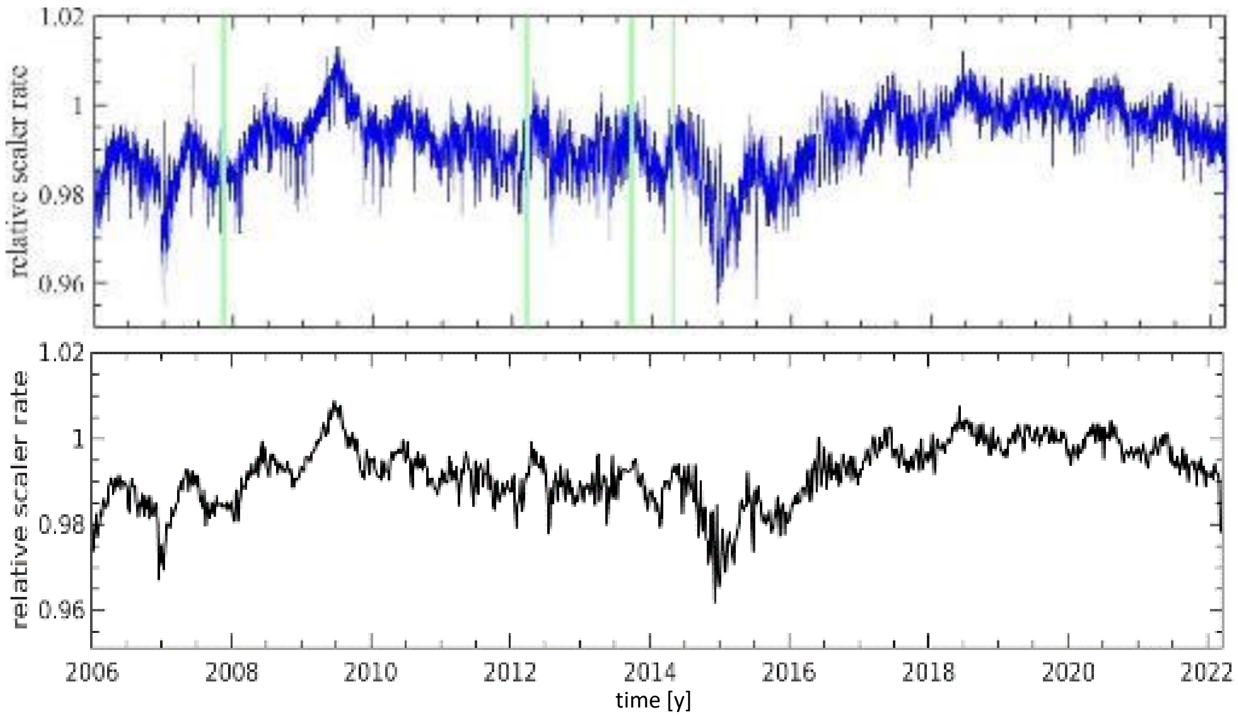


- Longer gaps occurring in 2007 (37 d), in 2012 (24 d), in 2013 (29 d), and in 2014 (19 d)
- All the gaps are filled using a gap-filling method relying on autoregressive (AR) models: missing data points are substituted with estimates derived from forward and backward AR fits of the remaining data samples

# ANNUAL CYCLE

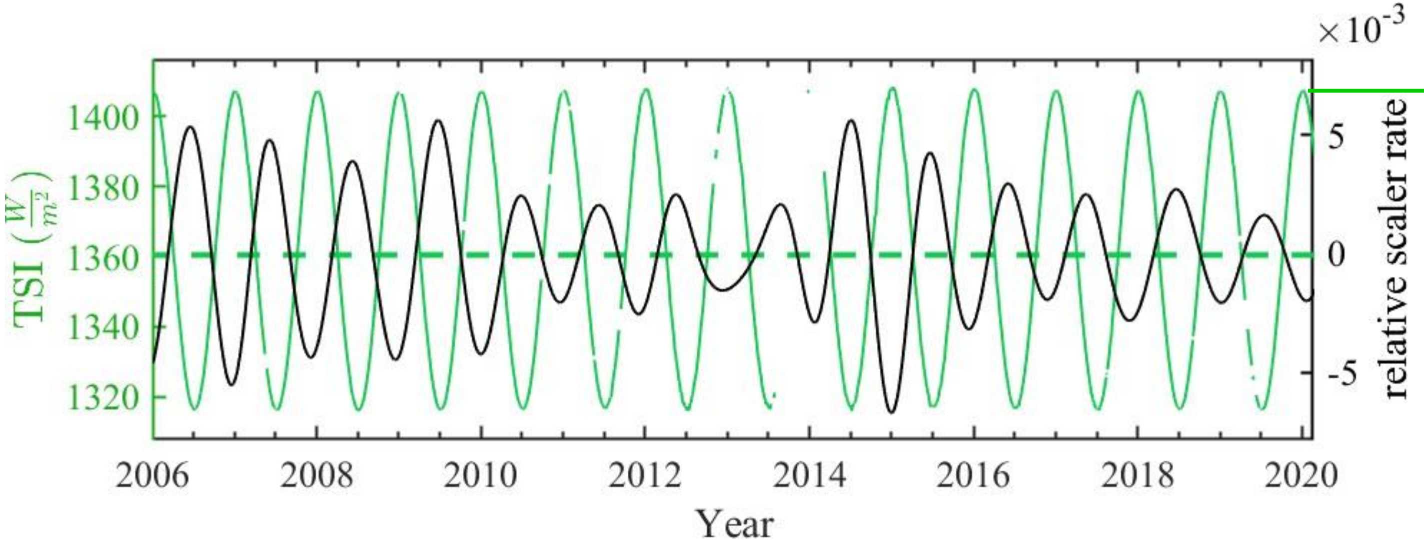


TSI = Total Solar Irradiance
(spatially and spectrally integrated solar radiation incident at the top of Earth's atmosphere)

Annual oscillation related to the variation of the Earth-Sun distance during the year

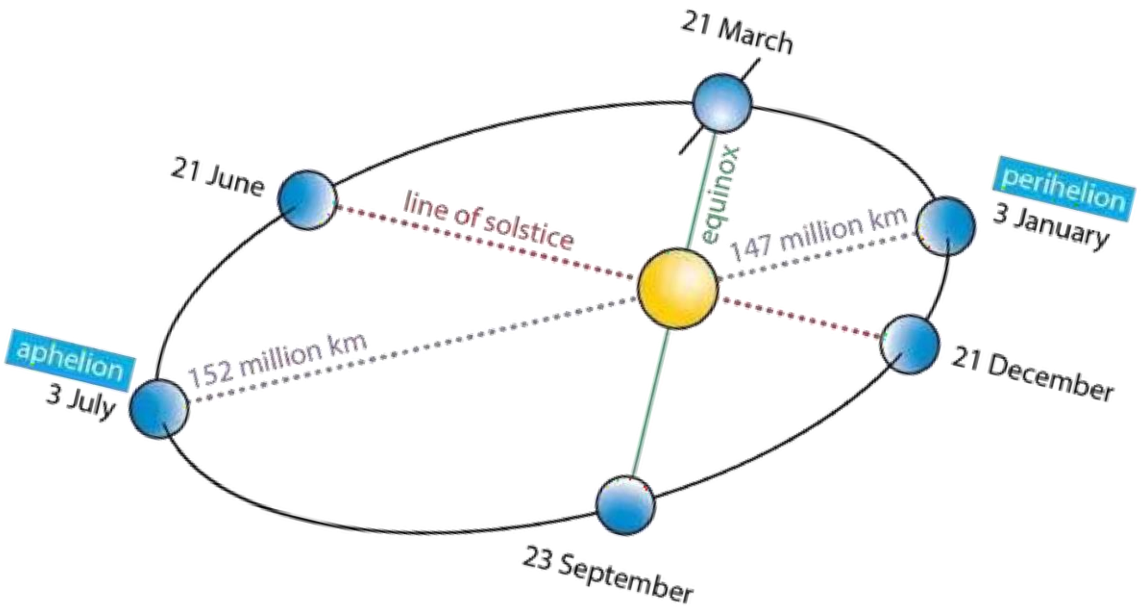


Shorter distance from the Sun (perihelion)

↓

More intense heliospheric magnetic field (lower GCR flux)

↓

Lower scaler rate values

Influence of temperature on scalers is currently under study

The annual component seems absent in the |B| series, but the distance R between ACE spacecraft and Sun during the year shows the same seasonal variation of the Earth-Sun distance

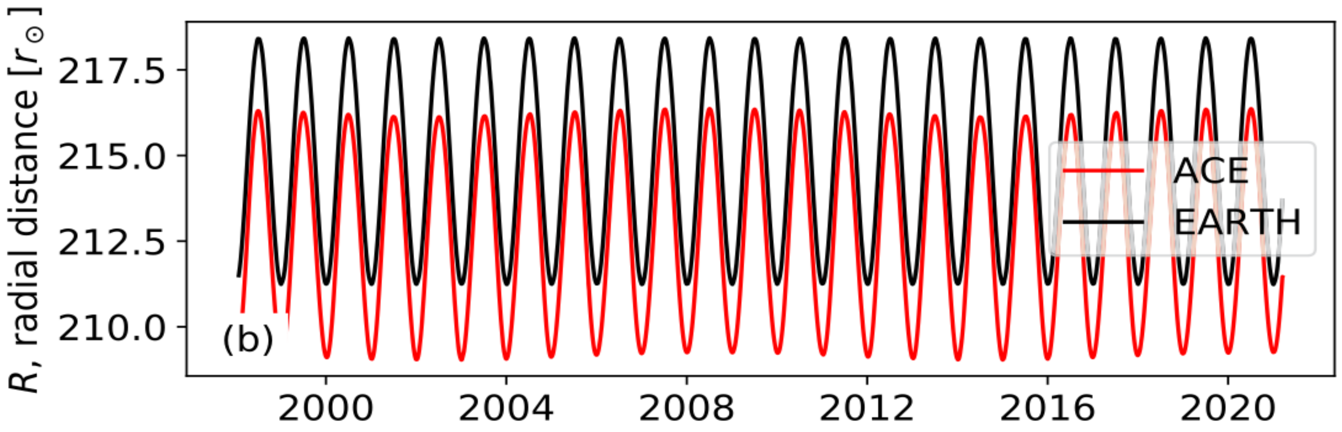


*Owens M.J., et. al.: Annual Variations in the Near-Earth Solar Wind, Solar Physics, 298, 111 (2023)*

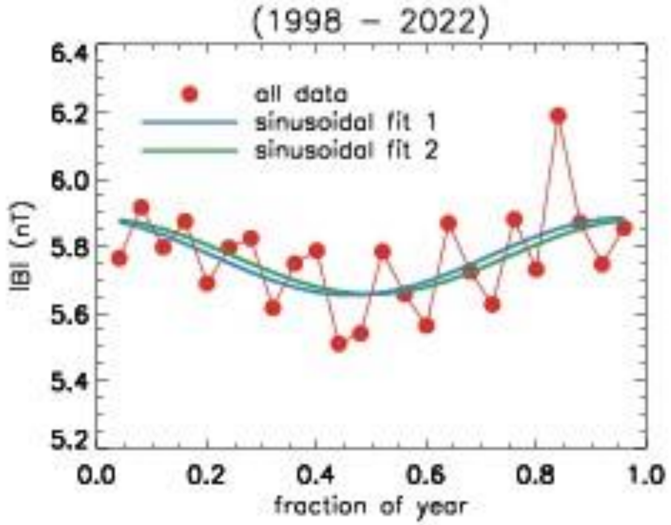


**We obtained an indication of the presence of the annual oscillation in the |B| series** by performing sinusoidal fits on the series, after having applied the *superposition of epochs method*

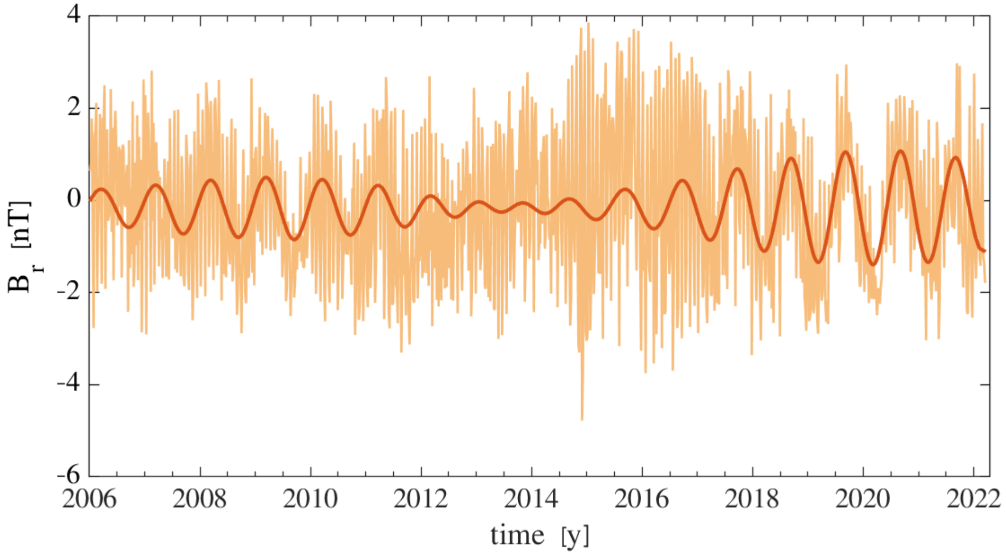


**Annual oscillation in the radial component $B_r$:** this indicates higher variability of the annual oscillation along the radial direction with respect to the HMF intensity

# MONTHLY AND SUB-MONTHLY MODULATIONS

**$\Delta t$ = 2 d**

**28-, ~14-, and 9-days components**: common origin

Detected in the time series of

- – HMF intensity |B|
- – HMF radial component $B_r$
- – coronal magnetic field at 2.50 $R_\odot$ ($B_{2.50\,R\odot}$)

SSA SIGNIFICANT COMPONENTS 99% c.l. – $\Delta t$ = 2d

| | SCALERS | \|B\| | $B_r$ | $B_{2.50\,R\odot}$ |
|---|---|---|---|---|
| Period | Variance [%] | | | |
| Trend (~11-y) | 64.2 | 17.0 | 1.4 | 3.4 |
| 1.2-y | - | 0.9 | - | - |
| 1-y | 10.7 | - | 5.9 | - |
| ~9-m | 1.9 | - | - | - |
| ~6-m | 1.5 | - | - | - |
| ~28-d | 2.2 | 2.8 | 30.9 | 47.9 |
| ~20-d | 0.3 | 0.7 | - | 1.6 |
| ~14-d | 0.7 | 4.9 | 13.4 | 32.4 |
| ~9-d | 0.3 | 7.4 | 6.2 | 9.4 |

| | | | | |
|---|---|---|---|---|
| SIGNAL | ~82% | ~34% | ~58% | ~95% |
| NOISE | ~18% | ~66% | ~42% | ~5% |

- Noise level in the $B_{2.50\,R\odot}$ much lower than those of |B| and $B_r$ series: being data extrapolated from the photospheric field, thus excluding the noise caused by transient solar activities
- Although the noise level observed in the scalers is higher than that of $B_{2.50\,R\odot}$ (due to the extrapolation of the latter), it results much lower than that in $B_r$ (of a factor 2) and in |B| (of a factor 3.7)
- This low noise level allows also to detect the two monthly oscillations not significant in the 3 magnetic field series

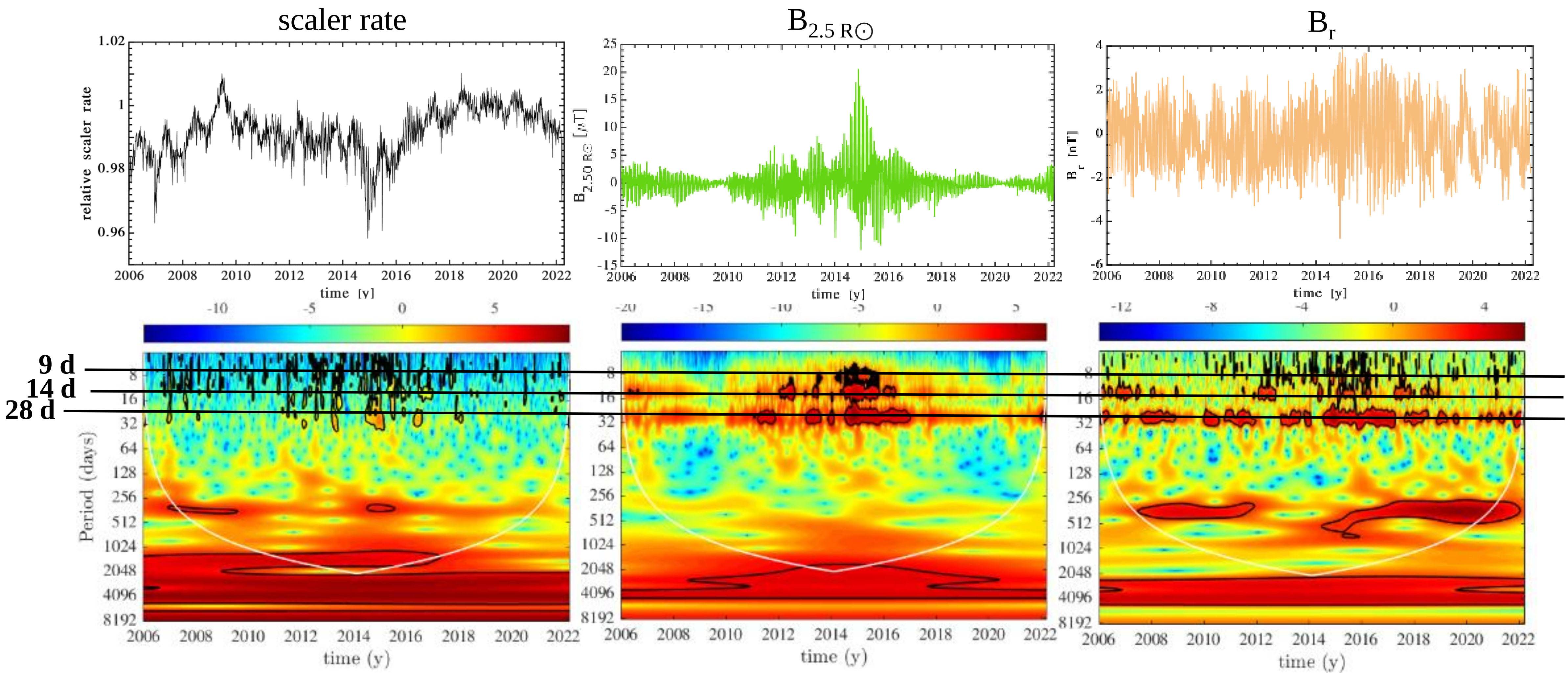


- Black lines: clear evidence of the 3 cycles, well distinguishable especially in the $B_{2.50\,R\odot}$ wav. spectrum
- These oscillations show higher and significant power during the solar maximum (2012–2018)
- Annual cycle: clearly seen in the scaler rate and $B_r$ time series (not in $B_{2.5\,R\odot}$ series as expected)
- Decadal cycle: present in all series

**The 28-days modulation** is caused by the combination of the **solar rotation** and an inhomogeneous distribution of long-lived solar active regions, e.g. sunspots, coronal holes and coronal mass ejections (CMEs).

**14-days** periodicity is linked to both solar active longitudes and tilted dipole structure was observed in several solar activity indices, as well as the monthly oscillation[1,2]

**9-d period** was associated with the distribution of coronal holes (CHs) appearing regularly spaced on the Sun over various solar rotations[3]

The 3 variabilities were also detected in the daily proton flux in cosmic rays[4], measured by the Alpha Magnetic Spectrometer (AMS) installed on the International Space Station (ISS)


[1] *López-Comazzi, Solar Phys., 295, 2020*

[2] Kalevi Mursula and Bertalan Zieger. "The 13.5-day periodicity in the Sun, solar wind, and geomagnetic activity: The last three solar cycles." *J. of Geoph. Res.: Space Physics* 101.A12 (1996)

3 M. Temmer *et al.* Periodic Appearance of Coronal Holes and the Related Variation of Solar Wind Parameters. *Sol Phys* **241**, 371–383 (2007)

[4] M. Aguilar et al. "Periodicities in the daily proton fluxes from 2011 to 2019 measured by the Alpha Magnetic Spectrometer on the International Space Station from 1 to 100 GV." *Phys. Rev. Lett.* 127.27 (2021)

[5] S. Prabhakaran Nayar *et al.* Short-Period Features of the Interplanetary Plasma and Their Evolution. *Sol Phys* **201**, 405–417 (2001)

RELATIVE SCALER RATE

| Null hypothesis | Significant components | Period | Variance (%) |
|---|---|---|---|
| AR(1) | 1,2 | Trend (~11 y) | 68.2 |
| AR(1) + RCs(1,2) | 3,4 | 1-y | 11.4 |
| AR(1) + RCs(1÷4) | 5,6 | 1-y | 3.4 |
| AR(1) + RCs(1÷6) | 7 | ~9-m | 1.0 |
| AR(1) + RCs(1÷7) | 8,9 | ~6-m | 1.6 |
| AR(1) + RCs(1÷9) | 11,12 | ~28-d | 0.9 |
| AR(1) + RCs(1÷9,11,12) | 17,18 | ~28-d | 0.6 |
| AR(1) + RCs(1÷9,11,12,17,18) | 20,21 | ~28-d | 0.6 |
| AR(1) + RCs(1÷9,11,12,17,18,20,21) | 41,42,43 | ~20-d | 0.4 |
| AR(1) + RCs(1÷9,11,12,17,18,20,21,41÷43) | 62,63 | ~14-d | 0.2 |
| AR(1) + RCs(1÷9,11,12,17,18,20,21,41÷43,62,63) | - | - | - |

SMF INTENSITY (|B|)

| Null hypothesis | Significant components | Period | Variance (%) |
|---|---|---|---|
| AR(1) | 1,2 | Trend (~11 y) | 37.9 |
| AR(1) + RCs(1,2) | 4,5 | ~14-d | 2.3 |
| AR(1) + RCs(1,2,4,5) | 3,6,9 | 1.2-y | 3.6 |
| AR(1) + RCs(1÷6,9) | 7,8 | ~14-d | 2.1 |
| AR(1) + RCs(1÷9) | 10,11 | ~28-d | 2.1 |
| AR(1) + RCs(1÷11) | 12,13 | ~14-d | 1.9 |
| AR(1) + RCs(1÷13) | 14,19 | ~9-m | 1.7 |
| AR(1) + RCs(1÷14,19) | 15,16 | ~28-d | 1.7 |
| AR(1) + RCs(1÷16,19) | 17,18 | ~28-d | 1.6 |
| AR(1) + RCs(1÷19) | 20,21 | ~20-d | 1.5 |
| AR(1) + RCs(1÷21) | 22,23 | ~28-d | 1.5 |
| AR(1) + RCs(1÷23) | 30,31 | ~4-m | 1.3 |
| AR(1) + RCs(1÷23,30,31) | - | - | - |

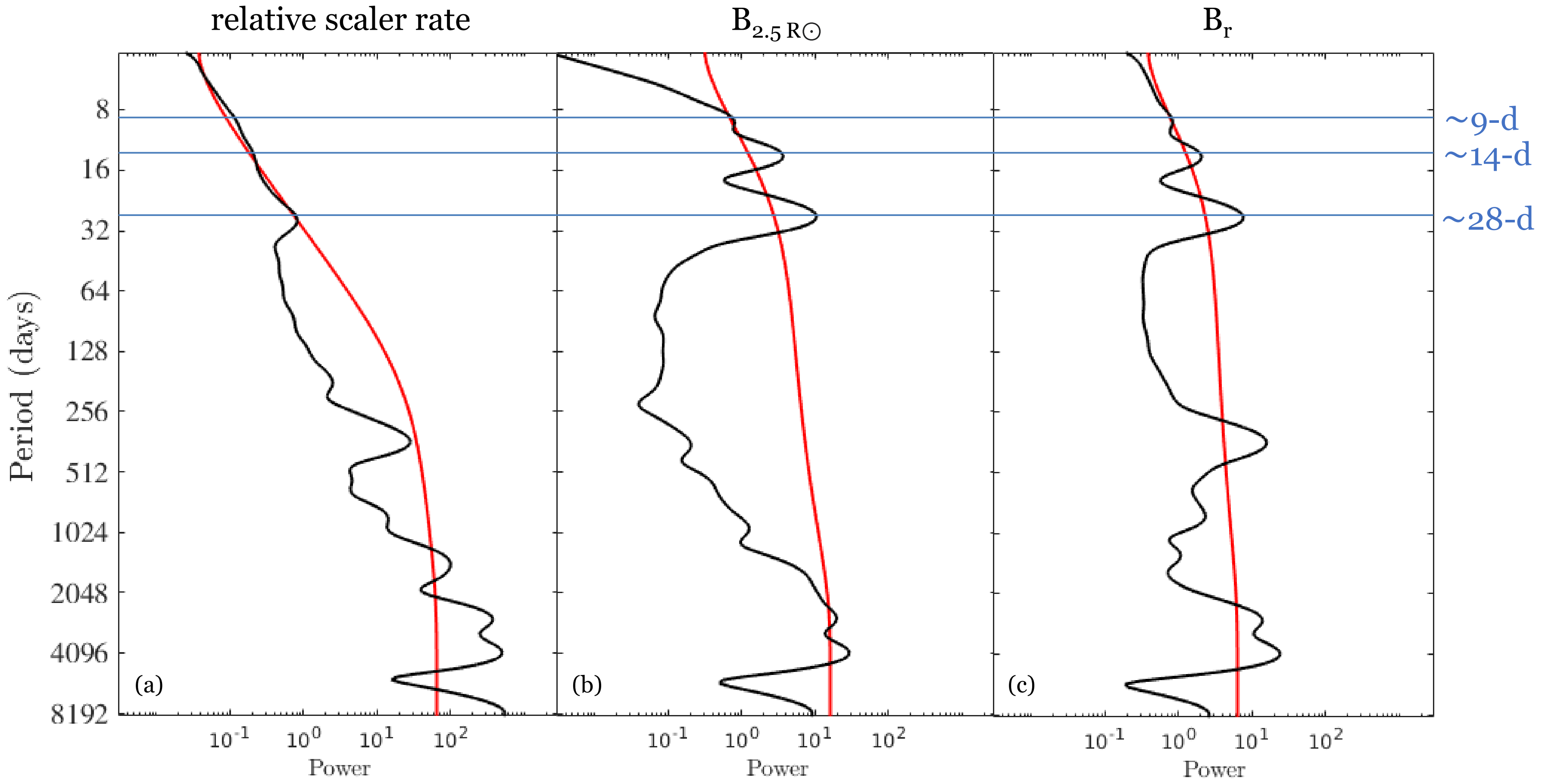
relative scaler rate
$B_{2.5\,R\odot}$
$B_r$
Period (days)
8
16
32
64
128
256
512
1024
2048
4096
8192
(a)
(b)
(c)
$10^{-1}$ $10^{0}$ $10^{1}$ $10^{2}$
Power
~9-d
~14-d
~28-d

# PROXIES OF SOLAR ACTIVITY
## (1) Sunspot number

- Archive of the SN series: World Data Center (WDC) - Sunspot Index and Long-term Solar Observations (SILSO), Royal Observatory of Belgium, Brussels.

- Daily data from 1818, monthly averages from 1749, and annual averages from 1700.

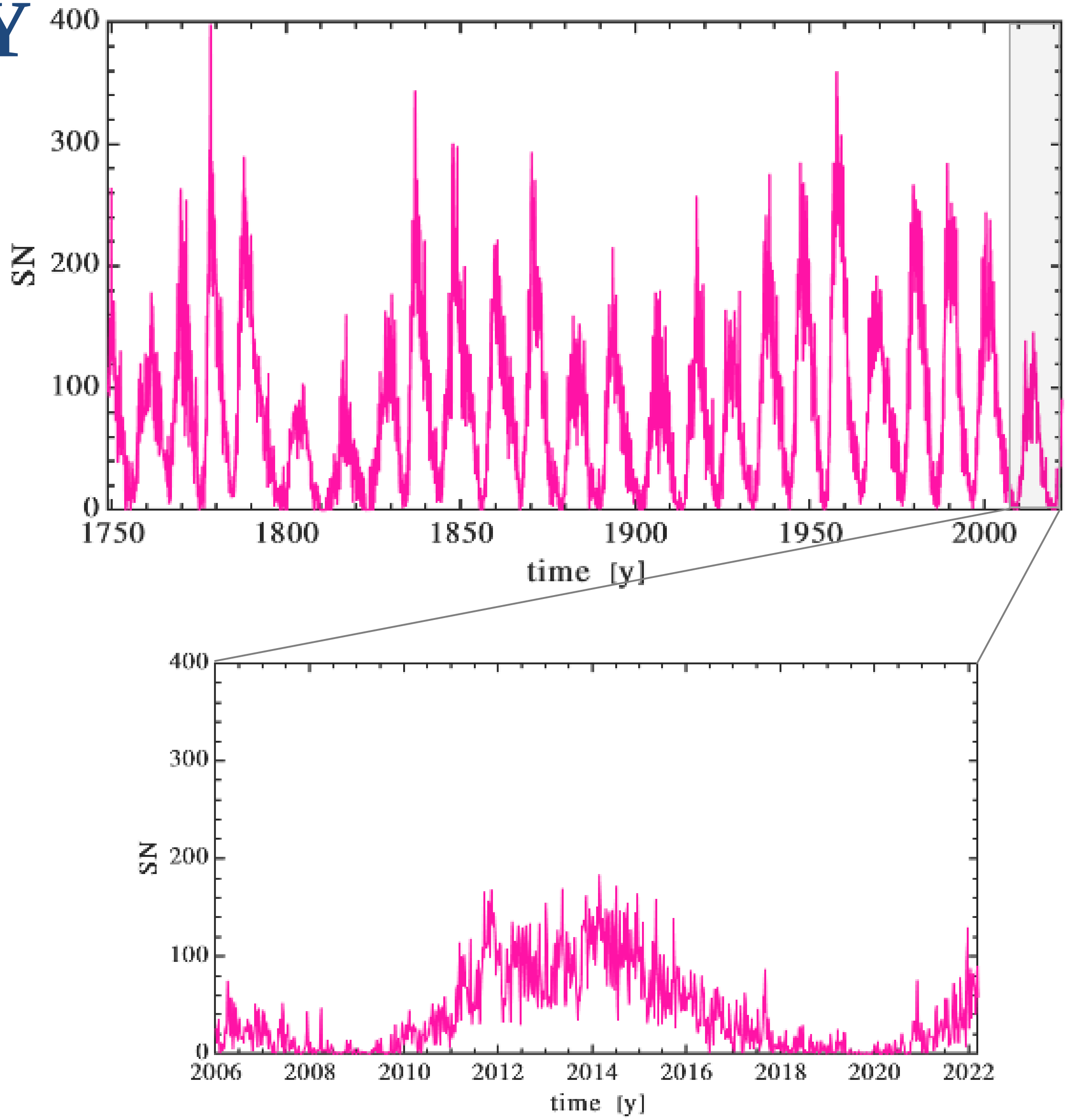

# PROXIES OF SOLAR ACTIVITY
## (2) Sunspot areas

- Archive of the sunspot areas series: United States Air Force (USAF) Solar Observing Optical Network (SOON), with the contribute of the US National Oceanic and Atmospheric Administration (NOAA).

- Daily data and monthly averages from 1874.

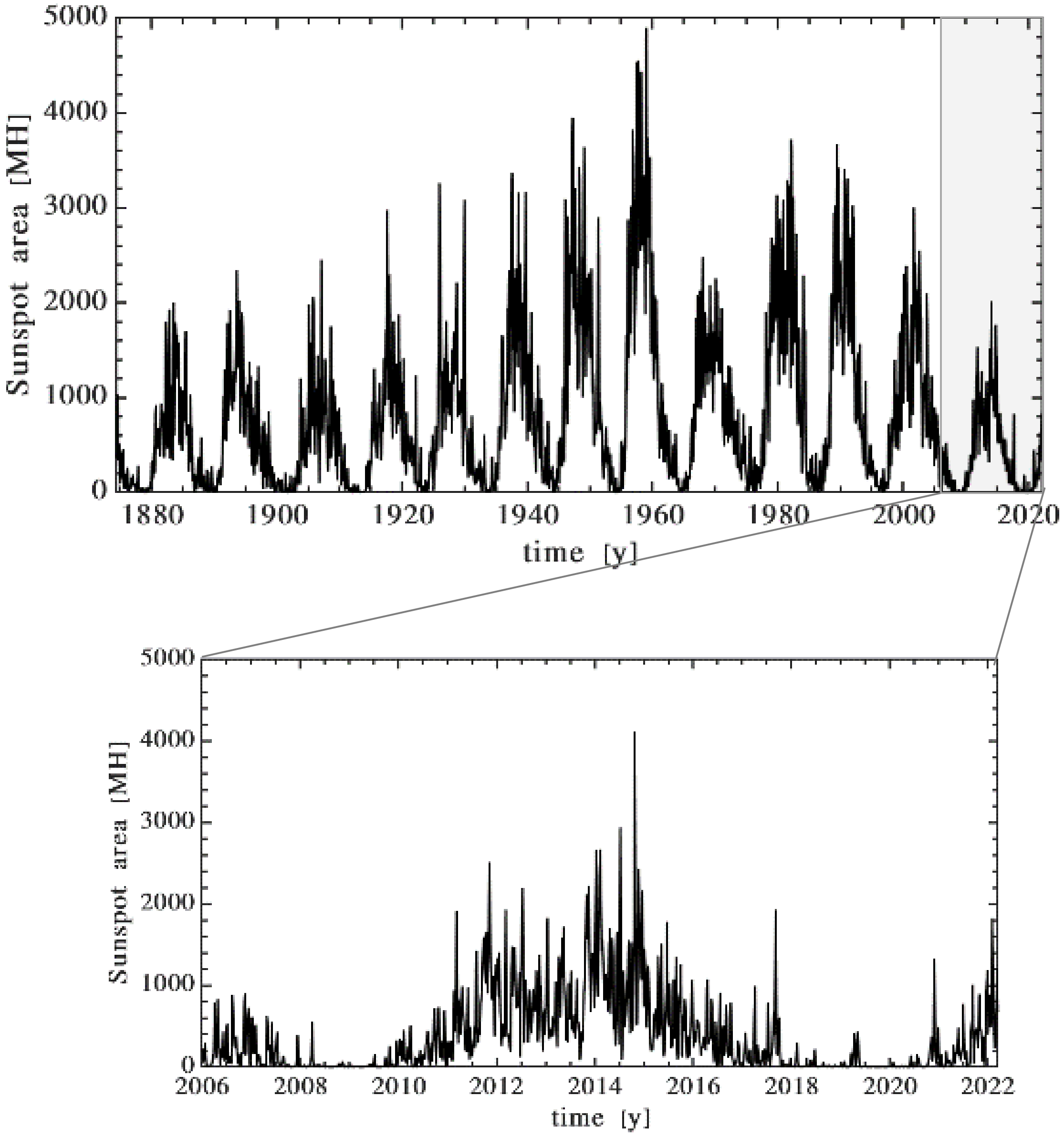

# Origin of the double peak (preliminary)

Mean sea level pressure shows the double peak (blue curve)

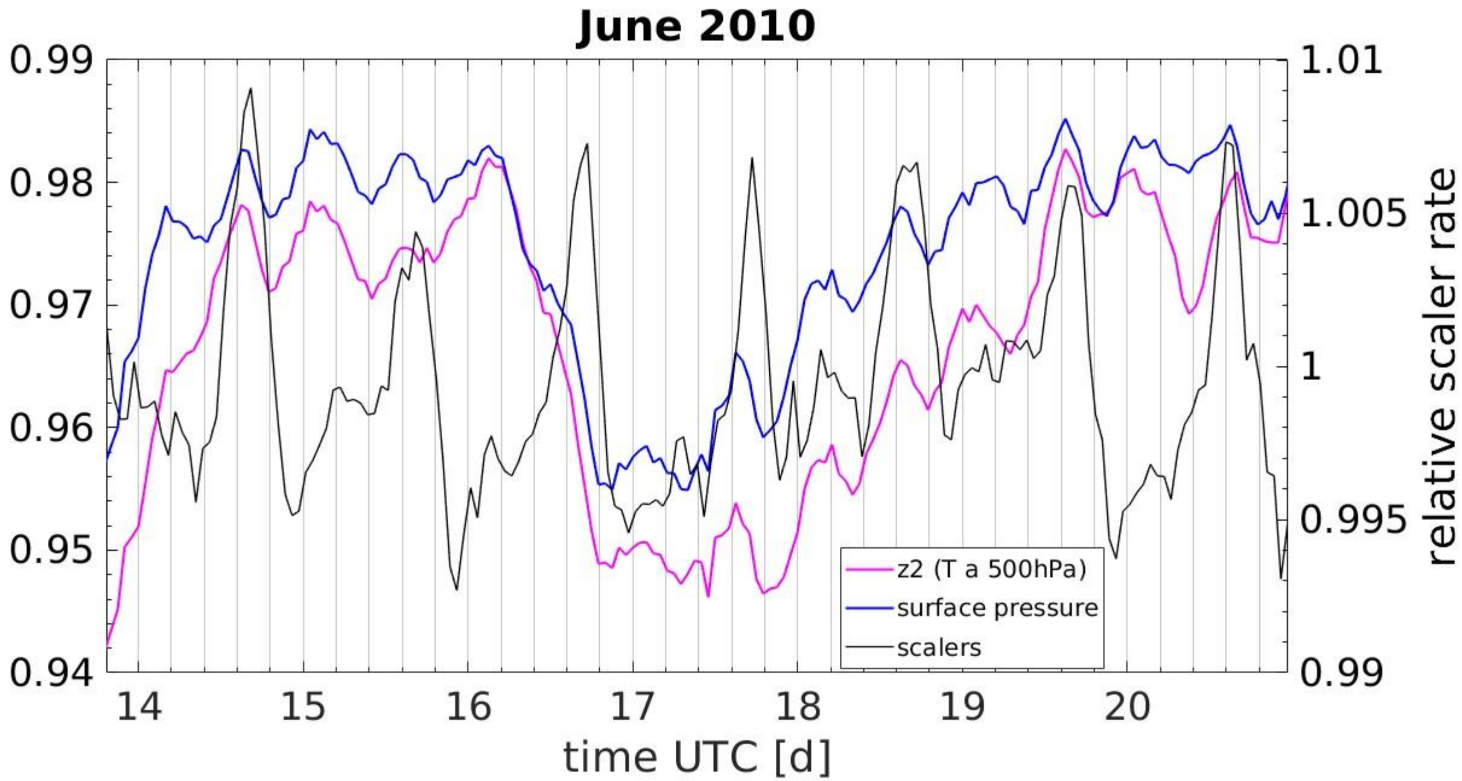


➡ **Is the scaler series well corrected for pressure?**

Using the hypsometric equation: z2 - z1 = (R * T / g) * ln(p1 / p2) z1 : Auger level, p1: surface pressure, p2: 500 hPa

we reveal a **density variation** with double peak (pink curve)

**Pressure/density variations may affect the scaler rate**

➡ **The correction could be efficient for long-term variations, but not for short-term variations**

# SINGULAR SPECTRUM ANALYSIS (SSA)

Characteristics of the SSA:

- separation of the deterministic components from the stochastic ones
- **data-adaptive basis functions (instead of fixed sinusoids as in fourier methods)**
- variance of the signal described by each component
- **Monte Carlo approach → statistical significance**

It involves 4 steps:

1. embedding the time series $\{X(t): t = 0, \dots N\}$ in a vector space of dimension $M$
2. computing the $MxM$ lag-covariance matrix $C_X$ of the data using the $N' x\, M$ trajectory matrix $D$ (with $N' = N - M + 1$)

$$D = \begin{pmatrix} X(1) & X(2) & \dots X(M) \\ \vdots & \vdots & \ddots \quad \vdots \\ X(N') & X(N'+1) & \dots X(N) \end{pmatrix} \qquad C_X = \frac{1}{N'} D^t D$$

where: $c_{ij} = \frac{1}{N-|i-j|} \sum_{t=1}^{N-|i-j|} X(t) X(t + |i - j|)$

3. diagonalizing $C_X$: determining eigenvectors $E_K$ and eigenvalues $\lambda_K$

- eigenvectors $E_K$ are definite variance directions
- eigenvalues $\lambda_K$ are the partial variance in the direction $E_K$

Projecting the time series onto each eigenvector $E_K$ yields the corresponding temporal principal components (PCs):

$$A_k(t) = \sum_{j=1}^{M} X(t+j) E_{\mathrm{j}}^{\ k}\,, \qquad t = 0, N - M$$

4. determining with a Monte Carlo test the significant components.

The final series will be the linear combination of the reconstructed components (RCs):

$$R_k(t) \ = c_t \sum_{k \epsilon K} \sum_{j=1}^{M} A_k(t-j) E_{\mathrm{j}}^{\ k} \qquad\qquad t = 1, N$$

where K is the set of significant components.

# CONTINUOUS WAVELET TRANSFORM (CWT)

This method provides a map in the *time-scale plane* which allows to study non-stationary features of the signal, such as:

→ changes in periodicity

→ isolated events

→ trends

→ intermittency

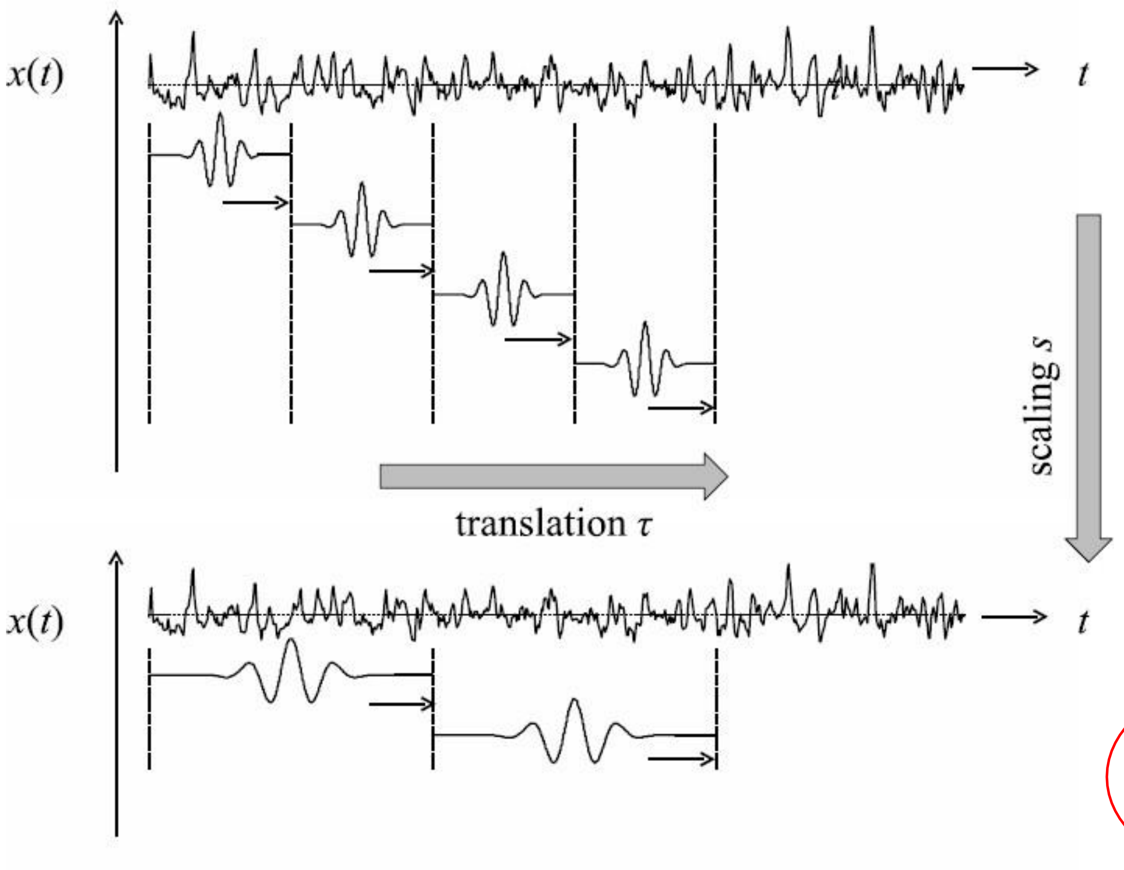


The CWT is defined by:

$$\boxed{W_x(a,\tau) = \frac{1}{\sqrt{a}}\int_{-\infty}^{+\infty} X(t)\, h\left(\frac{t-\tau}{a}\right) dt}$$

where:

- h(t) = mother wavelet
- a = dilation (scale) parameter
- τ =translation parameter

$\frac{\mathbf{1}}{\sqrt{\mathbf{a}}}\mathrm{h}\left(\frac{\mathbf{t-\tau}}{\mathbf{a}}\right)$ → Daughter wavelet = mother wavelet scaled (compressed or stretched)

The result is *a matrix of correlation values* describing the similarity between the signal and the daughter wavelet, at all considered scales and around each temporal location